

**Signal Transduction:**  
**Molecular Determinants of Allosteric  
Modulation at the M<sub>1</sub> Muscarinic  
Acetylcholine Receptor**



Alaa Abdul-Ridha, Laura López, Peter Keov,  
David M. Thal, Shailesh N. Mistry, Patrick M.  
Sexton, J. Robert Lane, Meritxell Canals and  
Arthur Christopoulos

*J. Biol. Chem.* 2014, 289:6067-6079.

doi: 10.1074/jbc.M113.539080 originally published online January 17, 2014

---

Access the most updated version of this article at doi: [10.1074/jbc.M113.539080](https://doi.org/10.1074/jbc.M113.539080)

Find articles, minireviews, Reflections and Classics on similar topics on the [JBC Affinity Sites](http://www.jbc.org/).

Alerts:

- [When this article is cited](#)
- [When a correction for this article is posted](#)

[Click here](#) to choose from all of JBC's e-mail alerts

This article cites 56 references, 28 of which can be accessed free at  
<http://www.jbc.org/content/289/9/6067.full.html#ref-list-1>

# Molecular Determinants of Allosteric Modulation at the M<sub>1</sub> Muscarinic Acetylcholine Receptor\*

Received for publication, December 2, 2013, and in revised form, January 16, 2014. Published, JBC Papers in Press, January 17, 2014, DOI 10.1074/jbc.M113.539080

Alaa Abdul-Ridha<sup>†1</sup>, Laura López<sup>‡</sup>, Peter Keov<sup>‡</sup>, David M. Thal<sup>‡</sup>, Shailesh N. Mistry<sup>§</sup>, Patrick M. Sexton<sup>‡2</sup>, J. Robert Lane<sup>‡</sup>, Meritxell Canals<sup>‡3</sup>, and Arthur Christopoulos<sup>‡2,4</sup>

From <sup>†</sup>Drug Discovery Biology and <sup>§</sup>Medicinal Chemistry, Monash Institute of Pharmaceutical Sciences and Department of Pharmacology, Monash University, Parkville, Victoria 3052, Australia

**Background:** BQCA is a selective allosteric modulator of the M<sub>1</sub> mAChR.

**Results:** Residues that govern BQCA activity were identified using mutagenesis and molecular modeling.

**Conclusion:** BQCA likely occupies a pocket overlapping prototypical mAChR modulators and gains selectivity through cooperativity with orthosteric ligands.

**Significance:** Understanding the structural basis of BQCA function can provide insight into the design of more tailored allosteric ligands.

Benzylquinolone carboxylic acid (BQCA) is an unprecedented example of a selective positive allosteric modulator of acetylcholine at the M<sub>1</sub> muscarinic acetylcholine receptor (mAChR). To probe the structural basis underlying its selectivity, we utilized site-directed mutagenesis, analytical modeling, and molecular dynamics to delineate regions of the M<sub>1</sub> mAChR that govern modulator binding and transmission of cooperativity. We identified Tyr-85<sup>2,64</sup> in transmembrane domain 2 (TMII), Tyr-179 and Phe-182 in the second extracellular loop (ECL2), and Glu-397<sup>7,32</sup> and Trp-400<sup>7,35</sup> in TMVII as residues that contribute to the BQCA binding pocket at the M<sub>1</sub> mAChR, as well as to the transmission of cooperativity with the orthosteric agonist carbachol. As such, the BQCA binding pocket partially overlaps with the previously described “common” allosteric site in the extracellular vestibule of the M<sub>1</sub> mAChR, suggesting that its high subtype selectivity derives from either additional contacts outside this region or through a subtype-specific cooperativity mechanism. Mutation of amino acid residues that form the orthosteric binding pocket caused a loss of carbachol response that could be rescued by BQCA. Two of these residues (Leu-102<sup>3,29</sup> and Asp-105<sup>3,32</sup>) were also identified as indirect contributors to the binding affinity of the modulator. This new insight into the structural basis of binding and function of BQCA can guide the design of new allosteric ligands with tailored pharmacological properties.

G protein-coupled receptors (GPCRs)<sup>5</sup> mediate a multitude of biological functions in response to a variety of ligands, including hormones and neurotransmitters, and play essential roles in all physiological processes (1). As such, GPCRs are important therapeutic targets for numerous diseases (2). Given such importance, an understanding of the structural basis underlying ligand binding and activation of GPCRs is essential to design more effective therapies (3). The recent surge in high resolution family A GPCR crystal structures (4) has provided new insights into the structural and functional diversity of this protein family. This knowledge, combined with information from computational, biochemical, and mutagenesis studies, has not only mapped out the location of orthosteric binding pockets but is starting to unravel the molecular changes that occur upon receptor activation and the mechanisms by which different ligands stabilize distinct conformational states (5, 6).

The M<sub>1</sub> mAChR is a family A GPCR and is one of five mAChR subtypes for which acetylcholine (ACh) is the endogenous orthosteric agonist. The ACh binding pocket is formed by amino acids that are conserved across all five mAChR subtypes and shares structural homology with other functionally unrelated acetylcholine-binding proteins from different species (7). Along with the M<sub>4</sub> mAChR, the M<sub>1</sub> mAChR is an attractive therapeutic target for the treatment of diseases in which cognition is impaired, such as Alzheimer disease and schizophrenia (8). However, because of the highly homologous ACh binding pocket across subtypes, it has been challenging to develop drugs that are sufficiently subtype-selective to avoid undesired activity at other mAChRs. This has spurred intensive efforts to discover allosteric ligands that act at topographically distinct regions on these receptors (9) with more potential to confer subtype selectivity. Despite the wealth of information obtained from GPCR crystal structures, challenges remain in understanding the mode of binding and action of such small molecule

\* This work was supported in part by National Health and Medical Research Council of Australia Program Grant 519461 (to A. C. and P. M. S.), Project Grant APP1011796 (to M. C.), and Grant APP1011920 (to J. R. L.) and computational studies were supported by Resource Allocation Scheme Grant VR0024 from the Victorian Life Sciences Computation Initiative, Peak Computing Facility, University of Melbourne.

<sup>†</sup> Recipient of an Australian Postgraduate Award scholarship.

<sup>‡</sup> Principal Research Fellows of the National Health and Medical Research Council of Australia.

<sup>3</sup> To whom correspondence may be addressed: Drug Discovery Biology, Monash Institute of Pharmaceutical Sciences, Monash University, 399 Royal Parade, Parkville, Victoria 3052, Australia. Tel.: 61-3-9903-9094; Fax: 61-3-9903-9581; E-mail: meri.canals@monash.edu.

<sup>4</sup> To whom correspondence may be addressed: Drug Discovery Biology, Monash Institute of Pharmaceutical Sciences, Monash University, 399 Royal Parade, Parkville, Victoria 3052, Australia. Tel.: 61-3-9903-9067; Fax: 61-3-9903-9581; E-mail: arthur.christopoulos@monash.edu.

<sup>5</sup> The abbreviations used are: GPCR, G protein-coupled receptor; BQCA, benzylquinolone carboxylic acid; ACh, acetylcholine; mAChR, muscarinic acetylcholine receptor; CCh, carbachol; QNB, quinuclidinyl benzilate; NMS, N-methylscopolamine; IP<sub>1</sub>, myo-inositol 1-phosphate; TM, transmembrane domain; ECL, extracellular loop; MD, molecular dynamics.

## Structure-Function Analysis of $M_1$ Receptor Allostery

allosteric modulators (9). High resolution structures of family A GPCRs bound to allosteric modulators are only starting to be solved (10), and even then the dynamic mechanisms contributing to modulator binding, receptor activation, and transmission of cooperativity between orthosteric and allosteric sites cannot be readily captured in a single structure.

The conserved ACh-binding site in mAChRs is located in the top third of the transmembrane helical bundle of the receptor with ACh contacting inward-facing residues in ECL2 and TMIII–VII (7, 11). In particular, TMIII contains a number of residues that have been implicated in both binding and activation mechanisms of the mAChRs and plays a central role as a structural and functional hub of many GPCRs (1). Accumulated evidence also points toward the existence of a “common” allosteric binding pocket utilized by structurally diverse mAChR allosteric modulators (12–14). This site is located within an extracellular “vestibule” and includes residues from both ECL2 and the extracellular regions of TMII and -VII (12, 13). Interestingly, we recently demonstrated that LY2033298, an allosteric modulator originally described as being a “selective” positive allosteric modulator for ACh at the  $M_4$  mAChR, can also occupy this conserved allosteric pocket at the  $M_2$  mAChR, where it exerts cooperative behavior with alternative orthosteric agonists, such as oxotremorine M, but not with ACh (14). Such probe dependence highlights the fact that selectivity of allosteric agents can actually be attained through two mechanisms, namely the differences in the allosteric site between receptor subtypes or the differences in cooperativity upon binding to a common allosteric site.

With regard to the  $M_1$  mAChR, several selective ligands have been discovered in the past few years (15). Among these, benzylquinolone carboxylic acid (BQCA) is a novel example of a highly selective positive allosteric modulator of ACh binding and function at the  $M_1$  mAChR, displaying very low affinity but a remarkably high cooperativity with ACh (16–18). The unprecedented subtype selectivity of BQCA thus suggests two potential scenarios as follows: (i) that BQCA binds to a completely different site than other mAChR allosteric modulators or (ii) that BQCA achieves subtype-selective cooperativity upon interaction with a conserved or overlapping allosteric site. In this study, we aimed to resolve this issue by site-directed mutagenesis of residues previously shown to be important for orthosteric, allosteric, or bitopic (dual orthosteric-allosteric) ligand binding at either the  $M_1$  mAChR or other mAChR family subtypes. Importantly, we also applied an analytical approach, based on the operational model of agonism (19, 20), to elucidate the effects of the introduced mutations on ligand binding *versus* signaling *versus* transmission of cooperativity. By doing so, we present new evidence for differential effects of distinct receptor regions on each of these molecular properties at the  $M_1$  mAChR.

### EXPERIMENTAL PROCEDURES

**Materials**—Chinese hamster ovary (CHO) FlpIn cells and Dulbecco’s modified Eagle’s medium (DMEM) were purchased from Invitrogen. Fetal bovine serum (FBS) was purchased from ThermoTrace (Melbourne, Australia). Hygromycin-B was purchased from Roche Applied Science. [ $^3$ H]Quinuclidinyl ben-

zilate ([ $^3$ H]QNB; specific activity, 50 Ci/mmol), *N*-[ $^3$ H]methylscopolamine ([ $^3$ H]NMS); specific activity, 85 Ci/mmol), and MicroScint scintillation liquid were purchased from PerkinElmer Life Sciences. IP-One assay kit and reagents were purchased from Cisbio (Codolet, France). All other chemicals were purchased from Sigma. BQCA was synthesized in-house at the Monash Institute of Pharmaceutical Sciences.

**Cell Culture and Receptor Mutagenesis**—Mutations of the c-Myc-hM $_1$  mAChR sequence were generated using the QuikChange site-directed mutagenesis kit (Agilent Technologies, La Jolla, CA). All mutations were confirmed by DNA sequencing (AGRF, Australia). Mutant c-Myc-hM $_1$  mAChR DNA constructs were transfected into FlpIn CHO cells (Invitrogen) and selected using 0.2 mg/ml hygromycin for stable expression.

**Whole Cell Radioligand Binding Assays**—To facilitate a more direct comparison between parameters derived from the analysis of cell-based functional assays (see below), radioligand binding experiments were performed on whole cells rather than membrane preparations. Saturation binding assays were performed using cells plated at  $10^4$  cells per well in 96-well Isoplates (PerkinElmer Life Sciences). The following day cells were incubated with the orthosteric antagonists [ $^3$ H]QNB or [ $^3$ H]NMS in a final volume of 100  $\mu$ l of HEPES buffer (10 mM HEPES, 145 mM NaCl, 1 mM MgSO $_4$ ·7H $_2$ O, 10 mM glucose, 5 mM KCl, 2 mM CaCl $_2$ , 1.5 mM NaHCO $_3$ , pH 7.4) for 2 h at room temperature. For competition binding assays, cells were plated at  $2.5 \times 10^4$  cells per well. The following day, cells were incubated in a final volume of 100  $\mu$ l of HEPES buffer containing increasing concentrations of the competing cold ligand CCh (in the absence or presence of increasing concentrations of BQCA) for 4 h at 4  $^\circ$ C (to avoid potential confounding effects of competing agonist ligands on receptor internalization while ensuring reactions reach equilibrium) in the presence of 0.3 nM [ $^3$ H]QNB or [ $^3$ H]NMS. Nonspecific binding was defined in the presence of 100  $\mu$ M atropine. For all experiments, termination of the assay was performed by rapid removal of radioligand followed by two 100- $\mu$ l washes with ice-cold 0.9% NaCl buffer. Radioactivity was determined by addition of 100  $\mu$ l of Microscint scintillation liquid (PerkinElmer Life Sciences) to each well and counting in a MicroBeta plate reader (PerkinElmer Life Sciences).

**IP-One Accumulation Assays**—The IP-One assay kit (Cisbio, France) was used for the direct quantitative measurement of myoinositol 1-phosphate (IP $_1$ ) in FlpIn CHO cells stably expressing either WT or mutant hM $_1$  mAChRs. This is a competitive immunoassay that measures the homogeneous time-resolved fluorescence signal transferred between a cryptate-labeled IP $_1$ -specific monoclonal antibody and  $d_2$ -labeled IP $_1$ . The fluorescence signal measured is inversely proportional to the concentration of native IP $_1$ .

Briefly, cells were seeded into 384-well proxy-plates at 7,500 cells per well and allowed to grow overnight at 37  $^\circ$ C, 5% CO $_2$ . The following day, cells were stimulated with CCh in IP $_1$  stimulation buffer (HEPES 10 mM, CaCl $_2$  1 mM, MgCl $_2$  0.5 mM, KCl 4.2 mM, NaCl 146 mM, glucose 5.5 mM, LiCl 50 mM, pH 7.4) in the absence or presence of increasing concentrations of BQCA and incubated for 1 h at 37  $^\circ$ C, 5% CO $_2$ . Cells were lysed by the

addition of homogeneous time-resolved fluorescence reagents, the cryptate-labeled anti-IP<sub>1</sub> antibody, and the  $d_2$ -labeled IP<sub>1</sub> analog prepared in lysis buffer, followed by incubation for 1 h at room temperature. The emission signals were measured at 590 and 665 nm after excitation at 340 nm using the Envision multilabel plate reader (PerkinElmer Life Sciences), and the signal was expressed as the homogeneous time-resolved fluorescence ratio:  $F = (\text{fluorescence}_{665 \text{ nm}}/\text{fluorescence}_{590 \text{ nm}}) \times 10^4$ . Experiments using WT  $M_1$  mAChR CHO FlpIn cells were performed in parallel each day.

**Computational Methods for the Model of the Ligand-Receptor Complex**—The sequence of the hM<sub>1</sub> mAChR was retrieved from the Swiss-Prot database. ClustalX software (21) was used to align the hM<sub>1</sub> mAChR sequence with the crystal structure of the nanobody-stabilized active state of the human  $\beta_2$  adreno-receptor (Protein Data Bank code 3POG) (22). Ballesteros-Weinstein numbering was used for residues in the TMs (23).

The structural model of the receptor was built using the Modeler Version 9.12 suite of programs (24), which yielded 10 candidate models. The conserved disulfide bonds between residues Cys-98<sup>3,25</sup> at the top of TMIII and the cysteine in the middle of the ECL2 as well as the one between Cys-391<sup>6,61</sup> and Cys-394<sup>7,29</sup> in ECL3 present in the template structure were also built and maintained as a constraint for geometric optimization. The best structure was selected from these candidates, according to the Modeler Discrete Optimized Protein Energy (DOPE) assessment score and visual inspection. The resulting receptor structure was optimized using the Duan *et al.* (25) force field and the general Amber force field, and HF/6–31G\*-derived restrained electrostatic potential atomic charges were used for the ligands (26).

Docking of the ligands was performed with MOE (Molecular Operating Environment, Chemical Computing Group, Inc.). CCh was docked manually into the receptor model with the protonated nitrogen interacting with Asp<sup>3,32</sup> and the carbamate group situated toward TMVI resembling the position of the ligands described in the mAChR crystal structures (Protein Data Bank code 3UON (7) and Protein Data Bank code 4DAJ (11)). The allosteric binding site of BQCA was generated using the Alpha site finder. Dummy atoms were created from the obtained  $\alpha$  spheres. BQCA docking was carried out using the Induced Fit protocol, with Alpha PMI placement and Affinity dG rescoring. One main BQCA pose was obtained at an allosteric site comprising residues from ECL2, ECL3, TMII, and TMVII at the extracellular surface of the  $M_1$  mAChR. The lowest energy conformation of this pose was selected and subjected to an energy minimization using MMFF94X force field. Molecular dynamics (MD) simulations of the final complex was performed with NAMD2.9 (27) package using the protocol described previously (28).

**Data Analysis**—All data were analyzed using Prism 6.01 (GraphPad Software, San Diego). Inhibition binding curves between [<sup>3</sup>H]QNB or [<sup>3</sup>H]NMS and unlabeled ligands were fitted to a one-site binding model (29). Binding interaction studies with allosteric ligands were fitted to the following allosteric ternary complex model, Equation 1 (30),

$$Y = \frac{B_{\max}[A]}{[A] + \left(\frac{K_A K_B}{\alpha'[B] + K_B}\right) \left(1 + \frac{[I]}{K_I} + \frac{[B]}{K_B} + \frac{\alpha[I][B]}{K_I K_B}\right)} \quad (\text{Eq. 1})$$

where Y is percentage (vehicle control) binding;  $B_{\max}$  is the total number of receptors; [A], [B], and [I] are the concentrations of radioligand, allosteric modulator, and the orthosteric ligand, respectively;  $K_A$ ,  $K_B$ , and  $K_I$  are the equilibrium dissociation constants of the radioligand, allosteric modulator, and orthosteric ligand, respectively.  $\alpha'$  and  $\alpha$  are the binding cooperativities between the allosteric modulator and radioligand and the allosteric ligand and orthosteric ligand, respectively. Values of  $\alpha$  (or  $\alpha'$ ) > 1 denote positive cooperativity; values < 1 (but > 0) denote negative cooperativity, and values = 1 denote neutral cooperativity.

Concentration-response curves for the interaction between the allosteric ligand and the orthosteric ligand in the various functional signaling assays were globally fitted to the following operational model of allostery and agonism, Equation 2 (20),

$$E = \frac{E_m(\tau_A[A](K_B + \alpha\beta[B]) + \tau_B[B]K_A)^n}{([A]K_B + K_A K_B + [B]K_A + \alpha[A][B])^n + (\tau_A[A](K_B + \alpha\beta[B]) + \tau_B[B]K_A)^n} \quad (\text{Eq. 2})$$

where  $E_m$  is the maximum possible cellular response; [A] and [B] are the concentrations of orthosteric and allosteric ligands, respectively;  $K_A$  and  $K_B$  are the equilibrium dissociation constant of the orthosteric and allosteric ligands, respectively;  $\tau_A$  and  $\tau_B$  are operational measures of orthosteric and allosteric ligand efficacy, respectively;  $\alpha$  is the binding cooperativity parameter between the orthosteric and allosteric ligand, and  $\beta$  denotes the magnitude of the allosteric effect of the modulator on the efficacy of the orthosteric agonist. In many instances, the individual model parameters of Equation 2 could not be directly estimated via the nonlinear regression algorithm by analysis of the functional data alone, due to parameter redundancy. To facilitate model convergence, we therefore fixed the equilibrium dissociation constant of each ligand to that determined from the whole cell binding assays. This practice assumes that the affinity determined in the whole cell binding assays is not significantly different from the “functional” affinity operative at the level of the signaling assay, which may not always be the case (31), and thus may lead to a systematic error in the estimate of the operational efficacy parameter,  $\tau$ . However, because only a single pathway (IP<sub>1</sub>) is being considered, the *relative* differences between  $\tau$  values remain valid for statistical comparison purposes.

All affinity, potency, and cooperativity values were estimated as logarithms (32), and statistical comparisons between values were by one-way analysis of variance using a Dunnett's multiple comparison post test to determine significant differences between mutant receptors and the WT  $M_1$  mAChR. A value of  $p < 0.05$  was considered statistically significant.

## RESULTS

To identify the location of the binding pocket of BQCA and to gain insight into its molecular mechanism of allosteric modulation at the  $M_1$  mAChR, residues from distinct locations

## Structure-Function Analysis of $M_1$ Receptor Allostery

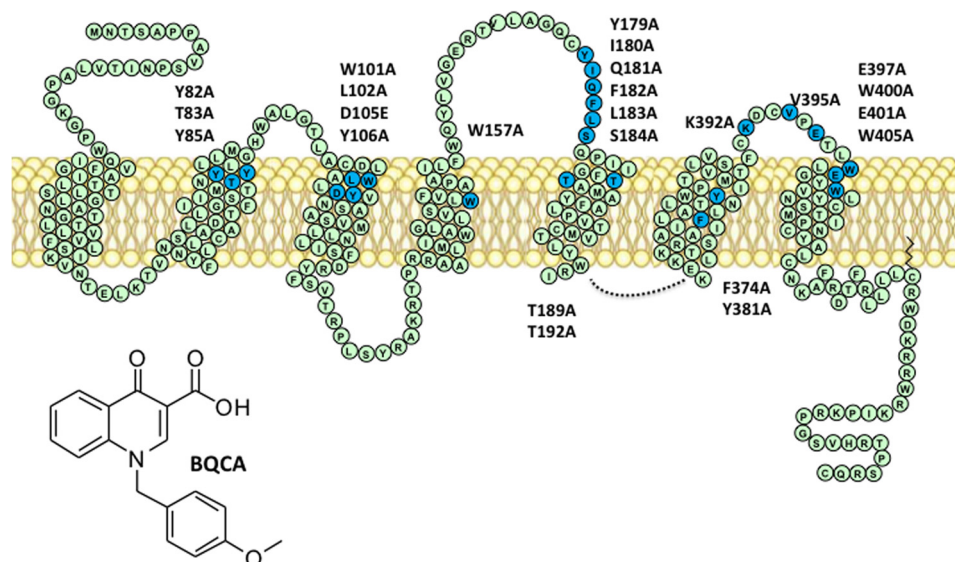


FIGURE 1. **Mutations and ligands investigated in this study.** A snake diagram of the human  $M_1$  mAChR highlighting mutated residues and chemical structure of the allosteric modulator BQCA.

within the receptor were mutated to alanine (Fig. 1). This includes residues previously shown to be important for orthosteric, allosteric, or bitopic ligand binding at either the  $M_1$  or other mAChR subtypes (18, 33–35).

**Effects of Amino Acid Substitutions on the Binding of Orthosteric Ligands at the  $M_1$  mAChR**—Whole cell [ $^3$ H]NMS saturation binding experiments showed that the majority of the mutations led to a significant reduction in cell surface receptor expression compared with the WT (Table 1). The maximum decrease in receptor expression relative to WT was 3-fold at F374<sup>6.44</sup>A. In agreement with previous reports (36, 37), no [ $^3$ H]NMS binding was detected when residues Tyr-106<sup>3.33</sup>, Trp-157<sup>4.57</sup>, Tyr-381<sup>6.51</sup>, or Val-395 were mutated to alanine. For these mutant receptors, [ $^3$ H]QNB was used as the alternative radioligand.

In addition to receptor expression, the equilibrium dissociation constant of orthosteric antagonists [ $^3$ H]NMS or [ $^3$ H]QNB ( $pK_A$ ) or the orthosteric agonist CCh ( $pK_I$ ) were significantly altered for a large number of mutants (Fig. 2 and Tables 1 and 2). Most notably, and in agreement with previous studies (33, 37, 38), alanine mutation of the TMII residues Tyr-82<sup>2.61</sup> or Tyr-85<sup>2.64</sup>, and the conserved orthosteric site residues Trp-101<sup>3.28</sup>, Leu-102<sup>3.29</sup>, Asp-105<sup>3.32</sup>, Tyr-106<sup>3.33</sup>, Trp-157<sup>4.57</sup>, Thr-189<sup>5.39</sup>, or Thr-192<sup>5.42</sup> caused significant reduction in the equilibrium dissociation constants of both CCh and the radiolabeled antagonist used (Fig. 2 and Tables 1 and 2). Mutation of Leu-183 in ECL2 or Val-395 in ECL3 also led to significant decreases in the affinities of both ligands. Consistent with previous findings showing that the Tyr-381<sup>6.51</sup> residue is able to discriminate between different mAChR antagonists (39, 40), we found that Y381<sup>6.51</sup>A completely abolished [ $^3$ H]NMS binding, although it showed unaltered affinity for [ $^3$ H]QNB. Several mutations showed differential effects between the binding of the radioligand and CCh. F182A and E397<sup>7.32</sup>A caused significant reduction in [ $^3$ H]NMS affinity but had no effect upon the affinity of CCh, whereas I180A and W400<sup>7.35</sup>A only decreased CCh affinity. Mutation of the highly conserved aromatic resi-

TABLE 1

### Whole cell equilibrium saturation binding parameters for WT and mutant $M_1$ mAChRs

Values represent the mean  $\pm$  S.E. from 2 to 5 separate experiments performed in duplicate.  $B_{\max}$  is the maximum density of binding sites per  $10^4$  cells in counts/min.  $pK_A$  is the negative logarithm of the radioligand equilibrium dissociation constant.

	$B_{\max}$	$pK_A$
$M_1$ WT [ $^3$ H]NMS	300 $\pm$ 10	10.04 $\pm$ 0.01
$M_1$ WT [ $^3$ H]QNB	290 $\pm$ 13	9.85 $\pm$ 0.03
Y82 <sup>2.61</sup> A	225 $\pm$ 7	9.76 $\pm$ 0.01 <sup>a</sup>
T83 <sup>2.62</sup> A	302 $\pm$ 5	9.95 $\pm$ 0.05
Y85 <sup>2.64</sup> A	398 $\pm$ 10	9.82 $\pm$ 0.03 <sup>a</sup>
W101 <sup>3.28</sup> A	177 $\pm$ 1 <sup>a</sup>	9.36 $\pm$ 0.06 <sup>a</sup>
L102 <sup>3.29</sup> A	147 $\pm$ 12 <sup>a</sup>	9.40 $\pm$ 0.05 <sup>a</sup>
D105 <sup>3.32</sup> E	195 $\pm$ 12 <sup>a</sup>	9.17 $\pm$ 0.07 <sup>a</sup>
Y106 <sup>3.33</sup> A <sup>b</sup>	220 $\pm$ 10	9.15 $\pm$ 0.20 <sup>a</sup>
W157 <sup>4.57</sup> A <sup>b</sup>	300 $\pm$ 8	9.32 $\pm$ 0.09 <sup>a</sup>
Y179A	270 $\pm$ 14	10.00 $\pm$ 0.02
I180A	186 $\pm$ 6 <sup>a</sup>	9.95 $\pm$ 0.03
Q181A	276 $\pm$ 8	9.92 $\pm$ 0.08
F182A	255 $\pm$ 7	9.52 $\pm$ 0.05 <sup>a</sup>
L183A	300 $\pm$ 23	9.31 $\pm$ 0.05 <sup>a</sup>
S184 <sup>3.32</sup> A	246 $\pm$ 9 <sup>a</sup>	10.04 $\pm$ 0.02
T189 <sup>5.39</sup> A	390 $\pm$ 13 <sup>a</sup>	9.56 $\pm$ 0.08 <sup>a</sup>
T192 <sup>5.42</sup> A	402 $\pm$ 12 <sup>a</sup>	9.76 $\pm$ 0.05 <sup>a</sup>
F374 <sup>6.44</sup> A	90 $\pm$ 8 <sup>a</sup>	9.29 $\pm$ 0.12 <sup>a</sup>
Y381 <sup>6.51</sup> A <sup>b</sup>	174 $\pm$ 15 <sup>a</sup>	9.82 $\pm$ 0.02
K392A	231 $\pm$ 7	9.88 $\pm$ 0.09
V395A <sup>b</sup>	315 $\pm$ 24	9.30 $\pm$ 0.06 <sup>a</sup>
E397 <sup>7.32</sup> A	237 $\pm$ 8 <sup>a</sup>	9.82 $\pm$ 0.02 <sup>a</sup>
W400 <sup>7.35</sup> A	138 $\pm$ 6 <sup>a</sup>	9.95 $\pm$ 0.01
E401 <sup>7.36</sup> A	236 $\pm$ 18 <sup>a</sup>	9.97 $\pm$ 0.05
W405 <sup>7.40</sup> A	189 $\pm$ 10 <sup>a</sup>	9.95 $\pm$ 0.02

<sup>a</sup> Data are significantly different ( $p < 0.05$ ) from WT value as determined by one-way analysis of variance with Dunnett's post hoc test.

<sup>b</sup> Experiments and statistical comparisons are relative to WT [ $^3$ H]QNB values.

dues Phe-374<sup>6.44</sup> and Trp-405<sup>7.40</sup> as well as the ECL2 residue Gln-181 resulted in substantially enhanced CCh binding affinity, with F374<sup>6.44</sup>A also displaying reduced [ $^3$ H]NMS binding. Mutation of Phe-374<sup>6.44</sup> and Trp-405<sup>7.40</sup> to alanine has been previously shown to cause constitutive receptor activity, which is likely to account for the increase in CCh affinity (38, 40–43). Alanine substitution of Tyr-179, Ser-184<sup>5.32</sup>, Lys-392, and Glu-401<sup>7.36</sup> did not impact the affinity of either agonist or antagonist. Overall, the change in  $pK_A$  of the radiolabeled antagonists tracks with changes in CCh  $pK_I$  for the majority of mutations

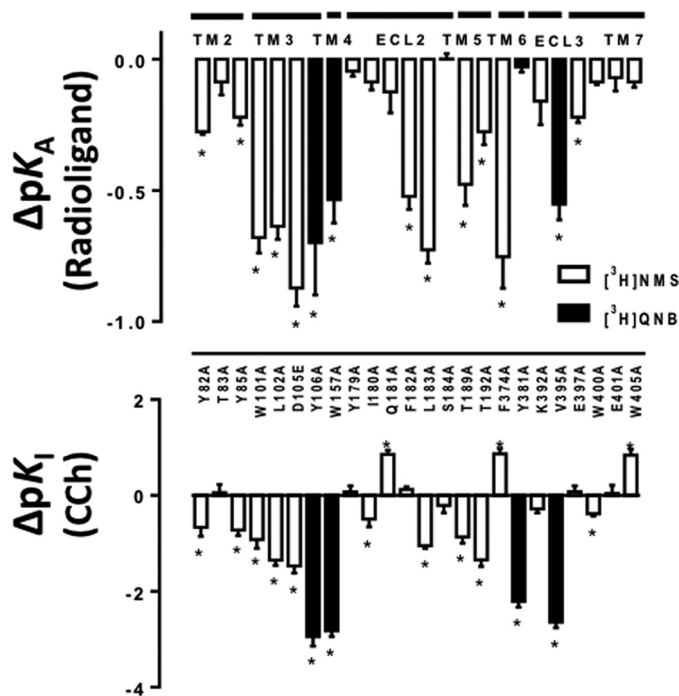


FIGURE 2. Orthosteric agonist affinity estimates are differentially modified by  $M_1$  mAChR mutations. Bars represent the difference in  $pK_A$  of orthosteric antagonist [ $^3H$ ]NMS or [ $^3H$ ]QNB (top panel) derived from whole cell saturation binding experiments (Table 1) or the difference in  $pK_1$  of the orthosteric agonist CCh (bottom panel) derived from whole cell competition binding experiments (Table 2), relative to the WT receptor value for each ligand at each mutant residue. Data represent the mean  $\pm$  S.E. of three experiments performed in duplicate. \*, significantly different from WT,  $p < 0.05$ , one-way analysis of variance, Dunnett's post hoc test.

tested (Fig. 2). Those that showed the most divergent effects include Y381<sup>6.51</sup>A in the orthosteric pocket, causing a marked decrease in CCh affinity but not that of [ $^3H$ ]QNB and Q181A, F374<sup>6.44</sup>A, and W405<sup>7.40</sup>A that caused an increased affinity for CCh.

**Effect of Amino Acid Substitution on BQCA Affinity and on the Transmission of Binding Cooperativity with CCh at the  $M_1$  mAChR**—The orthosteric binding pocket is formed by amino acids that are fully conserved across all five mAChR subtypes (7). However, although the importance of these residues for orthosteric ligand binding has been demonstrated in numerous studies and confirmed in our results, less is known about the role of these residues in the actions of allosteric ligands. Mutation of Trp<sup>3.28</sup> at the  $M_2$  and  $M_4$  mAChRs led to a significant reduction in affinity of the allosteric modulator LY2033298 and its binding cooperativity with ACh (14, 33). To determine whether BQCA behaves in a similar manner to LY2033298 at the equivalent residue in the  $M_1$  mAChR, we performed equilibrium binding studies for the interaction between CCh and BQCA at W101<sup>3.28</sup>A, as well as at other orthosteric pocket residues. An allosteric ternary complex model (Equation 1) was applied to the data to obtain estimates of BQCA affinity at each mutant ( $pK_B$ ), and its binding cooperativity with CCh ( $\log \alpha$ ) (representative examples of the analysis for different constructs are shown in Fig. 3, and all results are summarized in Fig. 4).

We found that the cooperativity of BQCA with CCh at W101<sup>3.28</sup>A, L102<sup>3.29</sup>A, or T192<sup>5.42</sup>A was not significantly different when compared with the WT receptor estimates (Fig. 4

TABLE 2

Whole cell equilibrium competition binding parameters for the interaction between [ $^3H$ ]NMS or [ $^3H$ ]QNB, CCh, and BQCA at the WT and mutant  $M_1$  mAChRs

Estimated parameter values represent the mean  $\pm$  S.E. of 3–4 experiments performed in duplicate and analyzed according to Equation 1.

	CCh $pK_1^a$	BQCA $pK_B^b$	$\log \alpha^c$
$M_1$ WT [ $^3H$ ]NMS	4.56 $\pm$ 0.05	4.49 $\pm$ 0.09	2.64 $\pm$ 0.12
$M_1$ WT [ $^3H$ ]QNB	4.67 $\pm$ 0.20	4.18 $\pm$ 0.18	2.31 $\pm$ 0.36
Y82 <sup>6.1</sup> A	3.89 $\pm$ 0.10 <sup>d</sup>	4.70 $\pm$ 0.08	2.53 $\pm$ 0.14
T83 <sup>2.62</sup> A	4.62 $\pm$ 0.12	4.39 $\pm$ 0.18	2.52 $\pm$ 0.24
Y85 <sup>2.64</sup> A	3.84 $\pm$ 0.08 <sup>d</sup>	4.32 $\pm$ 0.10	2.29 $\pm$ 0.13
W101 <sup>3.28</sup> A	3.64 $\pm$ 0.10 <sup>d</sup>	4.38 $\pm$ 0.06	2.43 $\pm$ 0.11
L102 <sup>3.29</sup> A	3.21 $\pm$ 0.06 <sup>d</sup>	4.12 $\pm$ 0.10 <sup>d</sup>	2.19 $\pm$ 0.12
D105 <sup>3.32</sup> E	3.09 $\pm$ 0.08 <sup>d</sup>	3.79 $\pm$ 0.07 <sup>d</sup>	1.61 $\pm$ 0.1 <sup>d</sup>
Y106 <sup>3.33</sup> A <sup>e</sup>	1.73 $\pm$ 0.10 <sup>d</sup>	ND <sup>f</sup>	ND
W157 <sup>4.57</sup> A <sup>e</sup>	1.85 $\pm$ 0.06 <sup>d</sup>	ND	ND
Y179A	4.63 $\pm$ 0.07	4.55 $\pm$ 0.11	0.52 $\pm$ 0.20 <sup>d</sup>
I180A	4.07 $\pm$ 0.08 <sup>d</sup>	5.03 $\pm$ 0.08 <sup>d</sup>	2.49 $\pm$ 0.13
Q181A	5.42 $\pm$ 0.05 <sup>d</sup>	5.12 $\pm$ 0.07 <sup>d</sup>	1.79 $\pm$ 0.1 <sup>d</sup>
F182A	4.68 $\pm$ 0.03	4.41 $\pm$ 0.07	1.79 $\pm$ 0.12 <sup>d</sup>
L183A	3.51 $\pm$ 0.03 <sup>d</sup>	4.23 $\pm$ 0.05	2.32 $\pm$ 0.08
S184 <sup>5.32</sup> A	4.35 $\pm$ 0.09	4.70 $\pm$ 0.1	2.27 $\pm$ 0.15
T189 <sup>5.39</sup> A	3.69 $\pm$ 0.07 <sup>d</sup>	4.68 $\pm$ 0.04	1.73 $\pm$ 0.11 <sup>d</sup>
T192 <sup>5.42</sup> A	3.22 $\pm$ 0.08 <sup>d</sup>	4.06 $\pm$ 0.13	2.18 $\pm$ 0.15
F374 <sup>6.44</sup> A	5.43 $\pm$ 0.08 <sup>d</sup>	5.38 $\pm$ 0.06 <sup>d</sup>	1.57 $\pm$ 0.15 <sup>d</sup>
Y381 <sup>6.51</sup> A <sup>e</sup>	2.46 $\pm$ 0.06 <sup>d</sup>	ND	ND
K392 <sup>6.62</sup> A	4.28 $\pm$ 0.05	4.40 $\pm$ 0.09	2.80 $\pm$ 0.12
V395 <sup>7.30</sup> A <sup>e</sup>	2.03 $\pm$ 0.06 <sup>d</sup>	4.31 $\pm$ 0.06	1.02 $\pm$ 0.25 <sup>d</sup>
E397 <sup>7.32</sup> A	4.64 $\pm$ 0.07	4.66 $\pm$ 0.07	1.79 $\pm$ 0.13 <sup>d</sup>
W400 <sup>7.35</sup> A	4.18 $\pm$ 0.02 <sup>d</sup>	ND	ND
E401 <sup>7.36</sup> A	4.60 $\pm$ 0.12	4.72 $\pm$ 0.08	1.74 $\pm$ 0.14 <sup>d</sup>
W405 <sup>7.40</sup> A	5.40 $\pm$ 0.07 <sup>d</sup>	5.70 $\pm$ 0.05 <sup>d</sup>	1.59 $\pm$ 0.12 <sup>d</sup>

<sup>a</sup> Negative logarithm of the equilibrium dissociation constant of CCh.

<sup>b</sup> Negative logarithm of the equilibrium dissociation constant of BQCA as estimated from Equation 1.

<sup>c</sup> Logarithm of the binding cooperativity factor between BQCA and CCh as estimated from Equation 1; for this analysis, the  $pK_A$  of the radiolabeled antagonist for the WT and each of the mutant receptors was constrained to the values listed in Table 1. The cooperativity between BQCA and the radioligand was constrained to  $-2$ , consistent with high negative cooperativity between the two ligands.

<sup>d</sup> Data are significantly different ( $p < 0.05$ ) from WT values as determined by one-way analysis of variance with Dunnett's post hoc test.

<sup>e</sup> Experiments and statistical comparisons are relative to WT [ $^3H$ ]QNB values.

<sup>f</sup> ND means not determined (no modulation of affinity).

and Table 2). Although these residues do not form direct contacts with orthosteric ligands, they have been described to constitute a "second shell" that stabilizes the primary binding pocket (3, 44). Interestingly, mutation of orthosteric binding site residues substantially affected the ability of BQCA to modulate CCh affinity; binding cooperativity with CCh was completely abolished at Y106<sup>3.33</sup>A, W157<sup>4.57</sup>A, and Y381<sup>6.51</sup>A and was significantly reduced at D105<sup>3.32</sup>E and T189<sup>5.39</sup>A (Figs. 3D and 4 and Table 2). In addition, V395A, which displayed a reduction in affinity for [ $^3H$ ]QNB and CCh similar to that of orthosteric site residues, also caused a significant reduction in binding cooperativity between BQCA and CCh (Table 2 and Fig. 4 (bottom panel)). No  $pK_B$  estimates for BQCA could be derived from the analysis of the binding interaction data of Y106<sup>3.33</sup>A, W157<sup>4.57</sup>A, or Y381<sup>6.51</sup>A due to the lack of allosteric modulation. The  $pK_B$  of BQCA was significantly lower than WT at L102<sup>3.29</sup>A and D105<sup>3.32</sup>E but was unchanged at the remaining orthosteric site mutations (Fig. 4 (top panel) and Table 2). These results suggest that residues that form direct contacts with the orthosteric ligand (7) also play a role in the transmission of cooperativity from the allosteric binding site of BQCA.

Equilibrium binding studies for the interaction between CCh and BQCA were also performed on residues previously described to participate in the allosteric modulation of mAChRs. Alanine

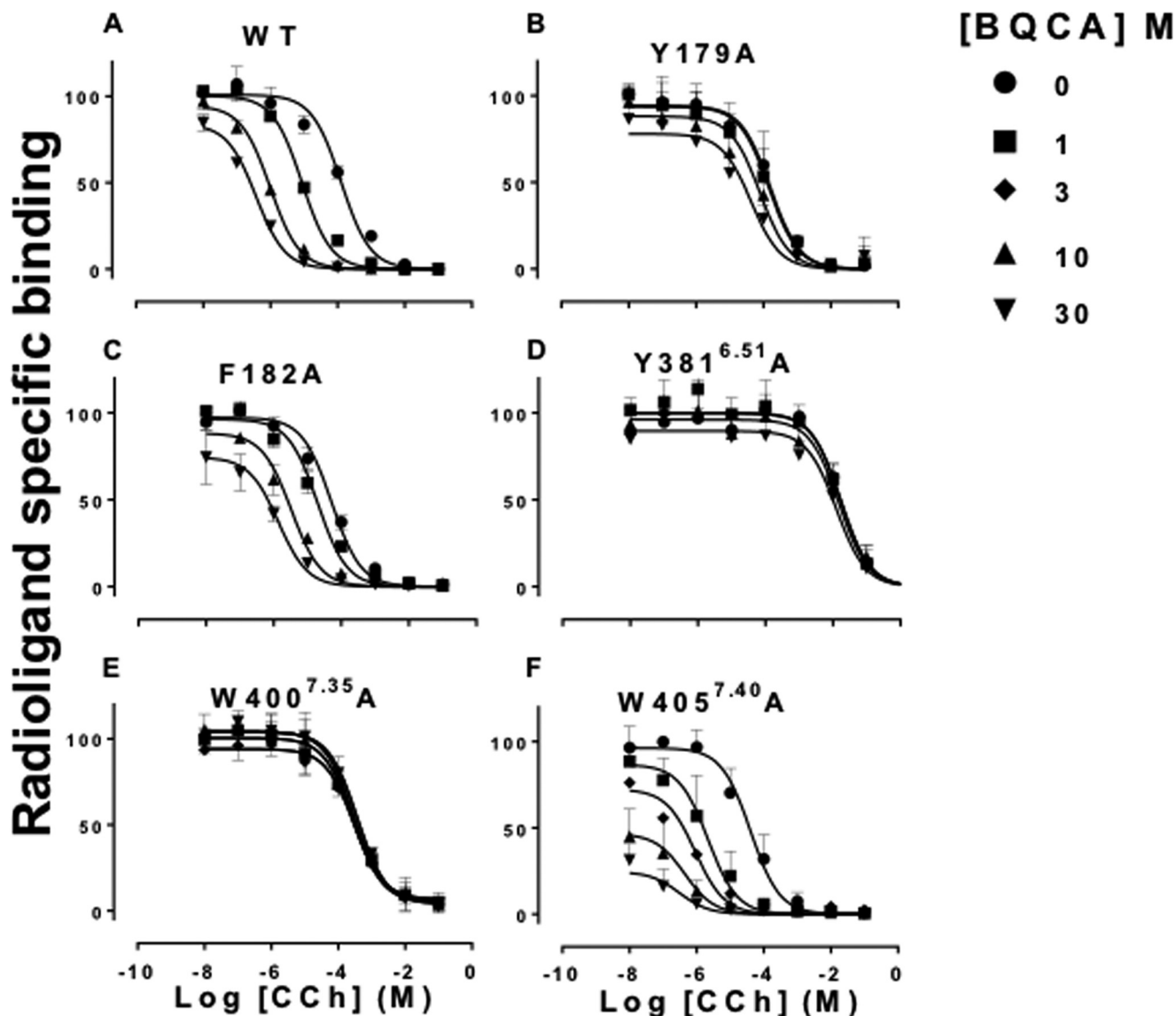


FIGURE 3. Identification of residues that differentially govern BQCA affinity and binding cooperativity with CCh at the  $M_1$  mAChR. The curves represent competition between [ $^3$ H]NMS (A–C, E, and F) or [ $^3$ H]QNB (D) and increasing concentrations of CCh in the absence or presence of varying concentrations of BQCA. All assays were performed using 0.3 nM [ $^3$ H]NMS or [ $^3$ H]QNB in whole cells expressing the WT or mutant c-Myc-tagged  $M_1$  mAChRs as described under “Experimental Procedures.” Data points represent the mean  $\pm$  S.E. of three independent experiments performed in duplicate. Curves drawn through the points in A–C and F represent the best fit of an allosteric ternary complex model (Equation 1). Parameters obtained from these experiments are listed in Table 2.

substitution of the TMII residues had no effect on the binding cooperativity between BQCA and CCh (Table 2). However, alanine substitution of the ECL2 residues Tyr-179, Gln-181, and Phe-182 significantly reduced the binding cooperativity, with Tyr-179 having the most profound effect (Fig. 3, B and C, and Table 2). The cooperativity was unaffected at the remaining ECL2 residues I180A, L183A, and S184A (Table 2). However, although I180A did not have a significant effect on cooperativity, it had significant opposing effects on the affinities of CCh and BQCA, with a decrease in the former and an increase in the latter (Figs. 2 and 4 and Table 2).

Mutation of the glutamate residues Glu-397<sup>7.32</sup> and Glu-401<sup>7.36</sup>, which have been implicated in the binding of allosteric ligands at the mAChRs (34, 45, 46), also caused significant reduction in the binding cooperativity (Table 2). Alanine substitution of the conserved Trp-400<sup>7.35</sup> residue in TMVII led to

complete loss of allosteric modulation even at the highest concentrations of BQCA (Fig. 3E and Table 2) confirming the importance of this residue for the binding of allosteric ligands at the  $M_1$  mAChR (18, 40, 47) and suggesting that this is likely to be a residue with which BQCA directly interacts.

Alanine substitution of the conserved aromatic residues Phe-374<sup>6.44</sup> or Trp-405<sup>7.40</sup> also led to substantial reductions in the binding cooperativity (Fig. 3F and Table 2). Interestingly all three mutations (Q181A, F374<sup>6.44</sup>A, and W405<sup>7.40</sup>A) that led to an increase in CCh affinity also caused an increase in BQCA affinity and a reduction in the binding cooperativity between the two ligands (Figs. 2, 3F, and 4 and Table 2). The  $pK_B$  estimates obtained from the binding interaction studies at the remaining mutants were not significantly different from WT (Fig. 4 and Table 2). Overall, the binding interaction studies revealed a significant correlation between the changes in affin-

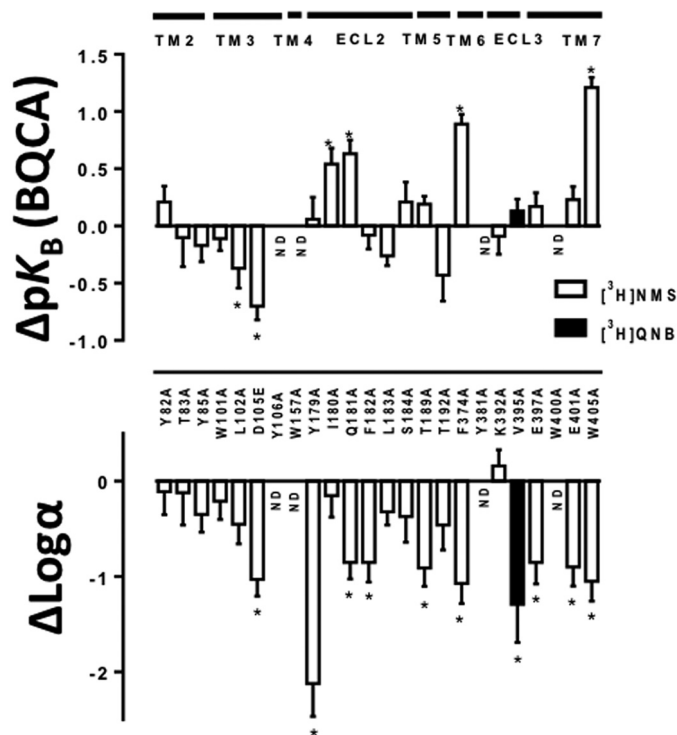


FIGURE 4. Effects of  $M_1$  mAChR mutations on BQCA affinity and binding cooperativity estimates. Bars represent the difference in  $pK_B$  (top panel) or binding cooperativity value ( $\log \alpha$ , bottom panel) of BQCA relative to WT as derived from binding interaction experiments with CCh (Table 2). Data represent the mean  $\pm$  S.E. of three experiments performed in duplicate. ND, no modulation by BQCA. \*, significantly different from WT,  $p < 0.05$ , one-way analysis of variance, Dunnett's post hoc test.

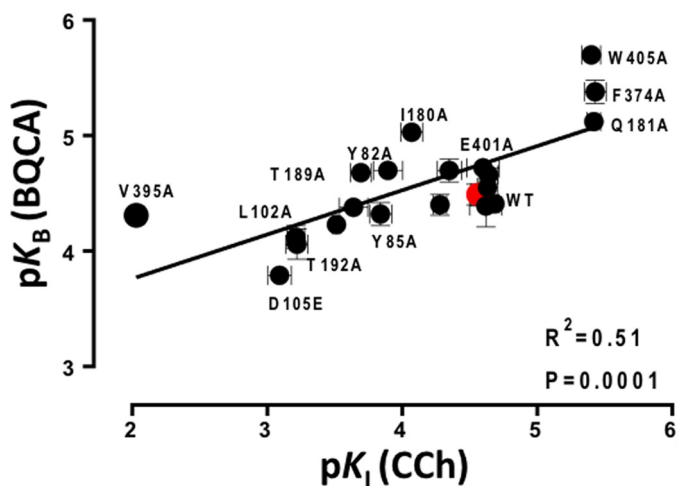


FIGURE 5. Positive correlation between the changes in orthosteric and allosteric ligand affinities at the  $M_1$  mAChR mutants. Each point represents the affinity values of BQCA ( $pK_B$ ) and CCh ( $pK_I$ ) as determined from whole cell competition binding studies as listed in Table 2.

ities of CCh and BQCA (Fig. 5). Additionally, these data show that residues located in both the putative allosteric and the orthosteric pockets are conformationally linked and contribute to the transmission of binding cooperativity.

*Effects of Mutations on Ligand Efficacy and on the Transmission of Functional Cooperativity between CCh and BQCA*—To investigate the effects of the selected mutations on the ability of BQCA to modulate signaling efficacy, we determined the concentration-response profile for CCh in the absence and pres-

TABLE 3  
CCh  $pEC_{50}$  and  $E_{max}$  values for WT and mutant  $M_1$  mAChRs as measured from the  $IP_1$  accumulation assay

Estimated parameter values represent the mean  $\pm$  S.E. of three experiments performed in duplicate.

	$pEC_{50}^a$	$E_{max}$
WT	$5.72 \pm 0.08$	100
Y82 <sup>2.61</sup> A	$4.65 \pm 0.20^b$	$66.03 \pm 7.35^b$
T83 <sup>2.62</sup> A	$5.27 \pm 0.15$	$20.39 \pm 1.35^b$
Y85 <sup>2.64</sup> A	$4.43 \pm 0.06^b$	$90.56 \pm 5.67$
W101 <sup>3.28</sup> A	$2.95 \pm 0.50^b$	$10.05 \pm 3.40^b$
L102 <sup>3.29</sup> A	$2.46 \pm 0.10^b$	$20.00 \pm 5.37^b$
D105 <sup>3.32</sup> E	NA <sup>c</sup>	NA
Y106 <sup>3.33</sup> A	NA	NA
W157 <sup>4.57</sup> A	NA	NA
Y179A	$4.39 \pm 0.14^b$	$82.38 \pm 4.47$
I180A	$4.43 \pm 0.27^b$	$79.92 \pm 9.37$
Q181A	$5.120 \pm 0.26$	$80.00 \pm 7.60$
F182A	$4.85 \pm 0.10^b$	$82.73 \pm 3.85$
L183A	$3.76 \pm 0.14^b$	$65.32 \pm 5.11^b$
S184 <sup>5.32</sup> A	$4.89 \pm 0.07^b$	$85.55 \pm 4.00$
T189 <sup>5.39</sup> A	$3.94 \pm 0.15^b$	$101.00 \pm 9.41$
T192 <sup>5.42</sup> A	$3.40 \pm 0.20^b$	$70.82 \pm 9.24$
F374 <sup>6.44</sup> A	$4.74 \pm 0.09^b$	$105.2 \pm 3.55$
Y381 <sup>6.51</sup> A	$3.10 \pm 0.30^b$	$21.81 \pm 3.00^b$
K392 <sup>6.62</sup> A	$5.37 \pm 0.12$	$91.19 \pm 5.66$
V395 <sup>7.30</sup> A	$4.71 \pm 0.11^b$	$97.23 \pm 4.45$
E397 <sup>7.32</sup> A	$5.50 \pm 0.21$	$96.20 \pm 8.89$
W400 <sup>7.35</sup> A	$3.50 \pm 0.08^b$	$71.80 \pm 3.70$
E401 <sup>7.36</sup> A	$5.12 \pm 0.05$	$99.00 \pm 3.39$
W405 <sup>7.40</sup> A	$5.21 \pm 0.05$	$84.38 \pm 1.98$

<sup>a</sup> Negative logarithm of the  $EC_{50}$  value.

<sup>b</sup> Significantly different ( $p < 0.05$ ), from WT value as determined by one-way analysis of variance with Dunnett's post hoc test.

<sup>c</sup> NA, not applicable (no detectable response).

ence of increasing concentrations of BQCA using  $IP_1$  accumulation as a canonical measure of  $M_1$  mAChR activation resulting from preferential activation of  $G_{\alpha_q}$  G proteins. The potency ( $pEC_{50}$ ) and maximal agonist effect ( $E_{max}$ ) parameters for CCh in the absence of modulator are shown in Table 3. As agonist potency is determined by affinity, signaling efficacy, and receptor density, we applied an operational model of allosterism (Equation 2 (20)) to estimate the effect of each mutation on the operational efficacy ( $\log \tau$ ) of CCh and BQCA without the confounding influence of affinity. The estimated  $\log \tau$  values were then corrected for changes in receptor expression and are summarized in Fig. 6 and Table 4. Additionally, analysis of the data with Equation 2 allowed for the estimation of the overall functional allosteric interaction between CCh and BQCA at each mutant (denoted by the parameter  $\log \alpha\beta$ ).

As summarized in Fig. 6 (representative examples in Fig. 7), the majority of the  $M_1$  mAChR mutations led to a significant reduction in the signaling efficacy of CCh ( $\log \tau_A$ ). Not surprisingly, the most prominent effects were seen for the orthosteric site residues in TMIII, W157<sup>4.57</sup>A in TMIV, and Y381<sup>6.51</sup>A in TMVI, consistent with reduced CCh affinity at these mutants and their importance for orthosteric ligand binding (3). No change in  $\log \tau_A$  was detected at residues for which CCh displayed higher affinity (Q181A, F374<sup>6.44</sup>A, and W405<sup>7.40</sup>A). Interestingly, our analysis indicated that the CCh  $\log \tau_A$  was significantly larger than WT at V395A in ECL3, despite a significant reduction in CCh binding affinity (Figs. 2 and 6 and Tables 1 and 2). BQCA agonism was not detected at any of the mutants with the exception of F374<sup>6.44</sup>A ( $\log \tau_B$   $0.55 \pm 0.10$ ) and W405<sup>7.40</sup>A ( $\log \tau_B$   $0.25 \pm 0.06$ ), where  $\log \tau_B$  was not significantly different to WT ( $\log \tau_B$   $0.38 \pm 0.05$ ) (Fig. 7).

## Structure-Function Analysis of $M_1$ Receptor Allostery

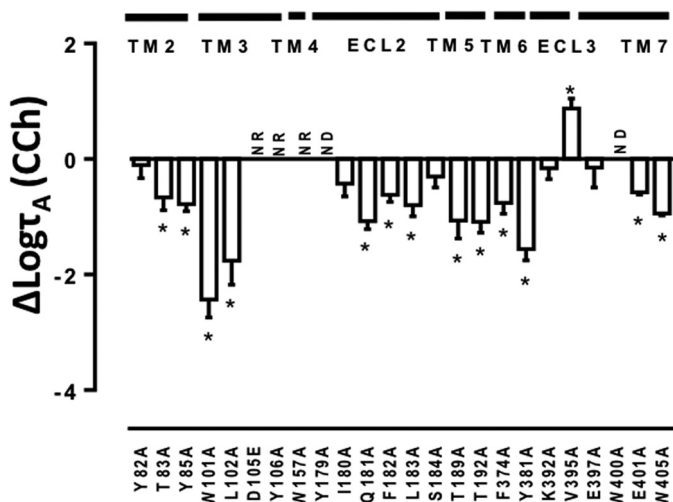


**FIGURE 6. CCh signaling efficacy ( $\log \tau_A$ ) estimates are differentially affected by  $M_1$  mAChR mutations.** Bars represent the difference in  $\log \tau_A$  of CCh at each mutant relative to the WT receptor value, as derived from application of the operational model of allostery to the  $IP_1$  interaction data at each mutant (Equation 2). Data represent the mean  $\pm$  S.E. of three experiments performed in duplicate. NR indicates that CCh activity was absent. ND indicates that Equation 2 could not be used due to loss of allosteric modulation by BQCA. \*, significantly different to WT receptor value,  $p < 0.05$ , one-way analysis of variance, Dunnett's post hoc test.

**TABLE 4**

**Operational model parameters for the functional allosteric interaction between CCh and BQCA at the WT and mutant  $M_1$  mAChRs measured using  $IP_1$  accumulation**

Estimated parameter values represent the mean  $\pm$  S.E. of three experiments performed in duplicate.  $\log \tau_A$  and  $\log \alpha\beta$  values were obtained from analyses of functional interaction data according to Equation 2. For this analysis, the  $pK_B$  and  $pK_B$  values for CCh and BQCA, respectively, were fixed to those determined from the radioligand binding assays as listed in Table 2.

	$\log \tau_A^a$	$\log \alpha\beta^b$
WT	1.32 $\pm$ 0.07	2.03 $\pm$ 0.12
Y82 <sup>2.61</sup> A	1.21 $\pm$ 0.13	1.14 $\pm$ 0.17 <sup>c</sup>
T83 <sup>2.62</sup> A	0.65 $\pm$ 0.13 <sup>c</sup>	0.73 $\pm$ 0.20 <sup>c</sup>
Y85 <sup>2.64</sup> A	0.53 $\pm$ 0.07 <sup>c</sup>	1.03 $\pm$ 0.09 <sup>c</sup>
W101 <sup>3.28</sup> A <sup>d</sup>	-1.11 $\pm$ 0.18 <sup>c</sup>	1.95 $\pm$ 0.17
L102 <sup>3.29</sup> A <sup>d</sup>	-0.44 $\pm$ 0.24 <sup>c</sup>	0.98 $\pm$ 0.15 <sup>c</sup>
D105 <sup>3.32</sup> E <sup>d</sup>	-0.69 $\pm$ 0.23 <sup>c</sup>	0.97 $\pm$ 0.20 <sup>c</sup>
Y106 <sup>3.33</sup> A <sup>d</sup>	-0.79 $\pm$ 0.21 <sup>c</sup>	1.24 $\pm$ 0.10 <sup>c</sup>
W157 <sup>4.57</sup> A <sup>d</sup>	-2.01 $\pm$ 0.20 <sup>c</sup>	1.74 $\pm$ 0.49
Y179A	ND <sup>e</sup>	ND
I180A	0.89 $\pm$ 0.13	1.35 $\pm$ 0.18
Q181A	0.24 $\pm$ 0.08 <sup>c</sup>	0.33 $\pm$ 0.12 <sup>c</sup>
F182A	0.70 $\pm$ 0.07 <sup>c</sup>	0.53 $\pm$ 0.13 <sup>c</sup>
L183A	0.52 $\pm$ 0.11 <sup>c</sup>	1.26 $\pm$ 0.13 <sup>c</sup>
S184 <sup>5.32</sup> A	1.01 $\pm$ 0.11	1.61 $\pm$ 0.14
T189 <sup>5.39</sup> A	0.25 $\pm$ 0.18 <sup>c</sup>	0.71 $\pm$ 0.12 <sup>c</sup>
T192 <sup>5.42</sup> A	0.23 $\pm$ 0.11 <sup>c</sup>	1.76 $\pm$ 0.10
F374 <sup>6.44</sup> A	0.56 $\pm$ 0.11 <sup>c</sup>	0.03 $\pm$ 0.02 <sup>c</sup>
Y381 <sup>6.51</sup> A <sup>d</sup>	-0.23 $\pm$ 0.11 <sup>c</sup>	1.25 $\pm$ 0.08 <sup>c</sup>
K392 <sup>6.62</sup> A	1.16 $\pm$ 0.11	1.92 $\pm$ 0.14
V395 <sup>7.30</sup> A	2.19 $\pm$ 0.10 <sup>c</sup>	1.46 $\pm$ 0.14
E397 <sup>7.32</sup> A	1.17 $\pm$ 0.20	1.07 $\pm$ 0.30 <sup>c</sup>
W400 <sup>7.35</sup> A	ND	ND
E401 <sup>7.36</sup> A	0.74 $\pm$ 0.02 <sup>c</sup>	0.93 $\pm$ 0.04 <sup>c</sup>
W405 <sup>7.40</sup> A	0.38 $\pm$ 0.02 <sup>c</sup>	0.47 $\pm$ 0.07 <sup>c</sup>

<sup>a</sup> Logarithm of operational efficacy parameter for CCh ( $\log \tau_A$ ) was corrected for changes in receptor expression to allow comparison with WT.

<sup>b</sup> Logarithm of the functional cooperativity between CCh and BQCA is shown.

<sup>c</sup> Significantly different ( $p < 0.05$ ), from WT value as determined by one-way ANOVA with Dunnett's post hoc test.

<sup>d</sup>  $pK_B$  of BQCA was left unconstrained at W101A, L102A, D105E, Y106A, W157A, and Y381A. The  $\log \tau_B$  of BQCA was constrained to -2 at these mutants.

<sup>e</sup> ND, no modulation by BQCA.

A common finding was obtained from the interaction studies between BQCA and CCh at the orthosteric site mutations that substantially impaired CCh signaling (W101<sup>3.28</sup>A, L102<sup>3.29</sup>A,

D105<sup>3.32</sup>E, Y106<sup>3.33</sup>A, W157<sup>4.57</sup>A, and Y381<sup>6.51</sup>A). As opposed to the loss of cooperativity between the two ligands seen in the binding interaction studies for the majority of these mutant receptors (Fig. 3D and Table 2), BQCA was able to rescue CCh function (Fig. 7D and Table 4). An analogous "rescue" of ACh function by LY2033289 has been described at equivalent TMIII residues in the  $M_4$  mAChR (33, 48). This finding indicates that a key part of the mechanism for the positive cooperativity mediated by BQCA on the orthosteric agonist involves a global drive of the receptor toward an active conformation.

The majority of mutant residues that displayed reduced binding cooperativity ( $\log \alpha$ ) between CCh and BQCA also caused a reduction in functional cooperativity ( $\log \alpha\beta$ ) between the two ligands (Fig. 8). These include the three residues that showed enhanced affinities for CCh and BQCA (Q181A, W405<sup>7.40</sup>A, and F374<sup>6.44</sup>A), F182A in ECL2 (Fig. 7, C and F), T189<sup>5.39</sup>A in TMV, and the two glutamate mutants E397<sup>7.32</sup>A and E401<sup>7.36</sup>A. The three residues mutated in TMII (Y82<sup>2.61</sup>A, T83<sup>2.62</sup>A, and Y85<sup>2.64</sup>A) and L183A in ECL2 caused significant reductions in functional cooperativity despite their lack of effect on binding cooperativity between CCh and BQCA (Fig. 8 and Table 4), indicating that these residues are likely to play a role in the transmission of functional cooperativity alone. In contrast, the  $\log \alpha\beta$  between BQCA and CCh at V395A was unchanged, despite significantly reduced binding cooperativity (Fig. 8 and Table 4). Consistent with the findings of Ma *et al.* (18), modulation of CCh efficacy was absent at Y179A and W400<sup>7.35</sup>A (Figs. 7, B and E, and 8). These results suggest that Trp-400<sup>7.35</sup> and Tyr-179 are likely to be residues with which BQCA directly interacts.

**Molecular Dynamics Simulations and Ligand Docking**—Ligand docking and molecular dynamic simulations were subsequently performed to rationalize our findings. This resulted in one main pose of BQCA in the predicted allosteric site.

The obtained complex for BQCA and CCh bound to the modeled  $M_1$  mAChR is shown in Fig. 9A. CCh forms the established salt bridge between the cationic nitrogen and Asp-105<sup>3.32</sup> and is fixed in a hydrophobic pocket formed by residues Tyr-106<sup>3.33</sup> in TMIII, Trp-157<sup>4.57</sup> in TMIV, Tyr-381<sup>6.51</sup> in TMVI, and Tyr-404<sup>7.39</sup> and Tyr-408<sup>7.43</sup> in TMVII (Fig. 9B). This is a signature network of interactions in cationic amine receptors (7, 11, 49), rhodopsins (51), and the adenosine  $A_{2A}$  receptor (52). Moreover, the orthosteric site is further flanked by the H-bonds formed between Tyr-106<sup>3.33</sup> and Tyr-381<sup>6.51</sup>, which adds stability to the binding pocket (3), and together with Tyr-404<sup>7.39</sup> and Tyr-408<sup>7.43</sup> formed an aromatic lid separating the orthosteric and allosteric pockets. The aromatic ring of Trp-157<sup>4.57</sup> appears to form a  $\pi$ - $\pi$  interaction with Tyr-106<sup>3.33</sup> (Fig. 9B), and it has been shown to form direct contact with the aromatic ring of the antagonist QNB (7).

The analysis of the MD trajectories shows the interaction of BQCA with residues located in the allosteric binding site (Fig. 9C). This binding site is defined by residues from TMII, TMVII, and ECL2 and is in agreement with our binding and functional studies; in particular, significant effects of the mutation of Tyr-179 in ECL2 and Trp-400<sup>7.35</sup> in TMVII can be reconciled with this pose. Tyr-179 is predicted to contribute to the stability of BQCA binding via formation of hydrophobic/edge-to-face  $\pi$ - $\pi$

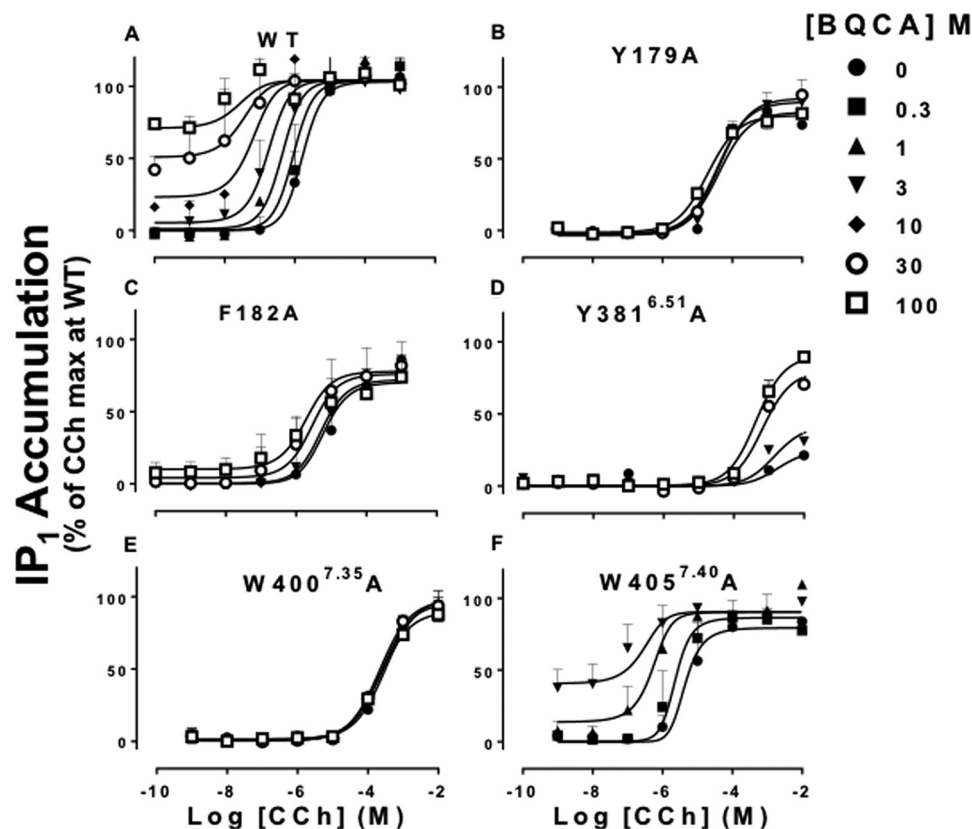


FIGURE 7. Identification of residues that differentially govern BQCA efficacy and functional cooperativity with CCh at the  $M_1$  mAChR. Interaction between BQCA and CCh in  $IP_1$  accumulation assay in CHO FlpIn cells stably expressing the WT or mutant  $M_1$  mAChRs. Data points represent the mean  $\pm$  S.E. of three independent experiments performed in duplicate. Curves drawn through the points in A, C, D, and F represent the best fit of an operational allosteric model (Equation 2 and Table 4) with the affinity of each ligand at each mutant fixed to the value determined from separate binding studies (Table 2).

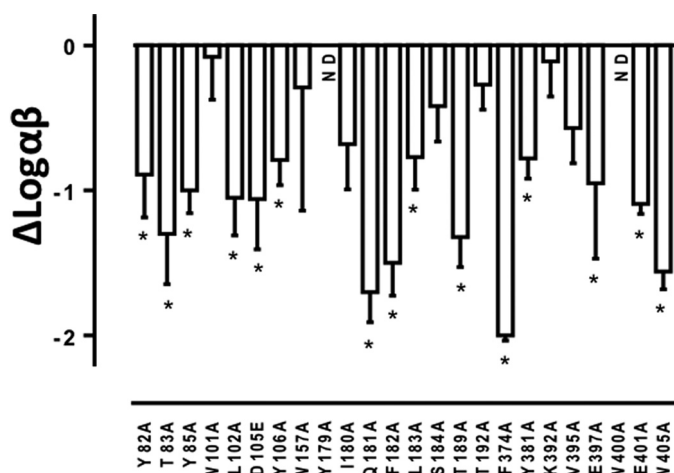


FIGURE 8. BQCA functional cooperativities are differentially modified by  $M_1$  mAChR mutations. Bars represent the difference in the functional cooperativity value ( $\log \alpha\beta$ , Equation 2) relative to the WT value, as derived from application of the operational model of allosterism to the CCh and BQCA  $IP_1$  interaction data at each mutant (Equation 2) (Table 4). Data represent the mean  $\pm$  S.E. from three experiments performed in duplicate. ND, no modulation by BQCA. \* significantly different from WT value,  $p < 0.05$ , one-way analysis of variance, Dunnett's post test.

interactions with both the bicyclic 4-oxoquinoline core and the benzylic pendant of BQCA. Similarly, Trp-400<sup>7.35</sup> is predicted to make a  $\pi$ - $\pi$  interaction with the benzylic pendant. In this model, Glu-397<sup>7.32</sup> also constrains this moiety of BQCA through a hydrophobic interaction, essentially forming a lid

over this part of the allosteric binding site. Tyr-85<sup>2.64</sup> and Tyr-82<sup>2.61</sup> are predicted to delimit the allosteric site via extra edge-to-face  $\pi$ - $\pi$ /hydrophobic interactions with the 4-oxoquinoline ring system (Fig. 9C). Although the former residue only affected the functional cooperativity between BQCA and CCh, it has been found to be an important contact residue for prototypical allosteric modulators at the  $M_2$  mAChR (13). Mutation of an adjacent residue at the  $M_4$  mAChR (I93<sup>2.65</sup>T) was found to be important for the transmission of cooperativity between ACh and LY2033298 (34), suggesting a contribution of this residue to a conserved allosteric pocket within the mAChR family. Fig. 10 shows the global movements of the ECLs and TMs as well as the movements of the residues to accommodate the binding of BQCA. These include the rotation of the aromatic side chains of Trp-400<sup>7.35</sup> (Fig. 10, inset) and Trp-405<sup>7.40</sup> that may be facilitating the accompanying shifts in the nearby TMVII residues Glu-397<sup>7.32</sup> and Glu-401<sup>7.36</sup> to constrain BQCA into the observed pose. The binding of BQCA also causes subtle movements in the ECLs; the most significant of these appear to be in ECL2 where the aromatic side chains of Tyr-179 and Phe-182 both move closer to BQCA, whereas Gln-181 adopts a horizontal position away from the ligand accessible cavity. These results support our finding that mutation of Glu-397<sup>7.32</sup>, Glu-401<sup>7.36</sup>, Tyr-179, and Phe-182 lead to reduced cooperativity between BQCA and CCh and that mutation of Gln-181 enhances the binding affinity of both ligands.

## Structure-Function Analysis of $M_1$ Receptor Allostery

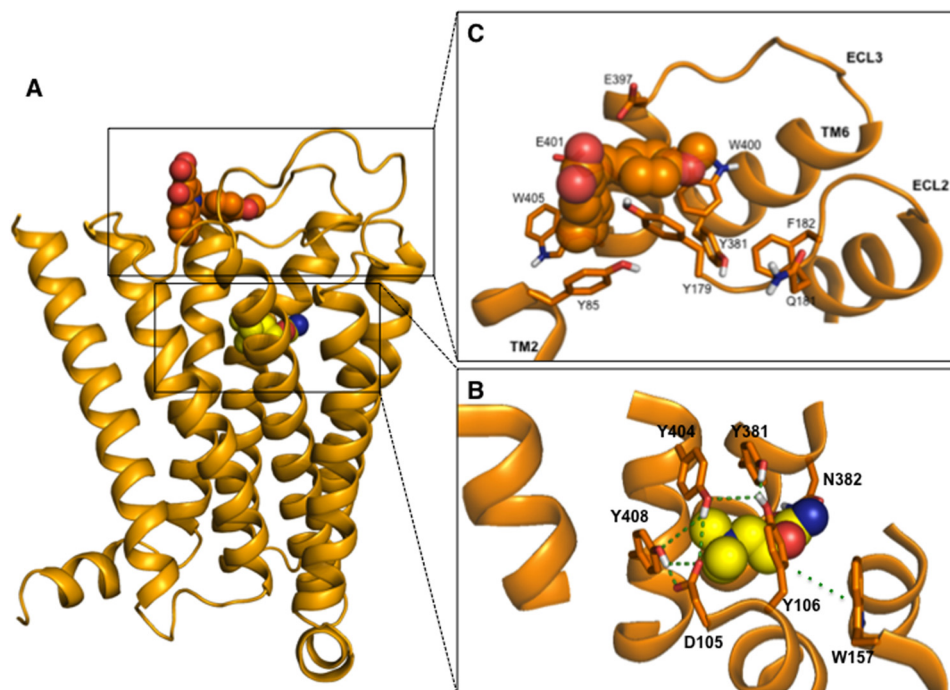


FIGURE 9. **Structural model of the  $M_1$  mAChR in complex with BQCA and CCh.** *A*, overall view of the complex obtained using MD simulations. The ligands are shown in orange (BQCA) and yellow (CCh) spheres. *B*, orthosteric binding site for CCh; *C*, predicted allosteric binding site of BQCA. Important residues are shown by orange sticks.

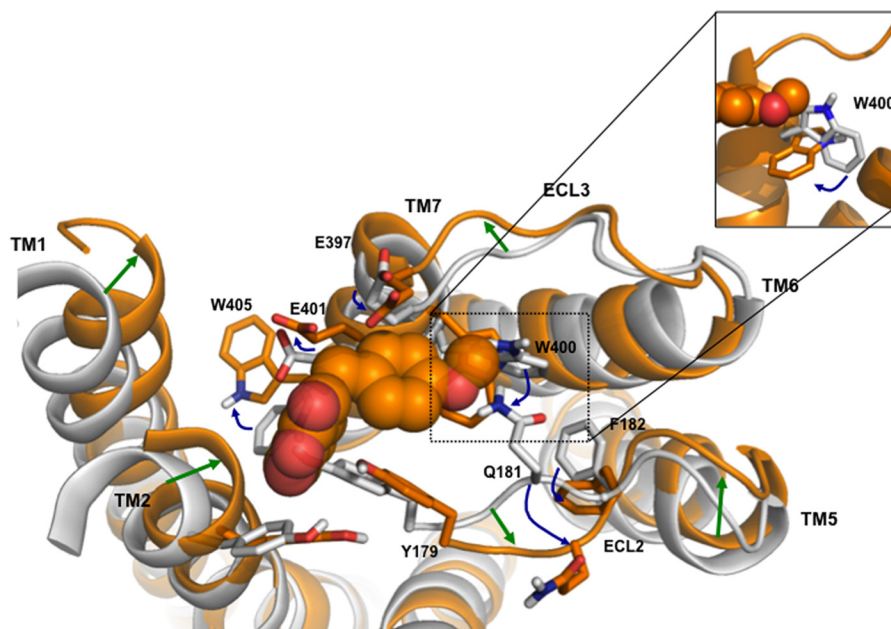


FIGURE 10. **Proposed rearrangement of ECLs and TMs upon BQCA binding to  $M_1$  mAChR.** Extracellular view of the BQC-binding site at the starting position for MD simulations (gray) or at the final position of the receptor after 20 ns of MD (orange). Important residues involved in BQCA binding or cooperativity are shown as sticks. Global movements of TMs and ECLs are shown with green arrows, and residue shifts are indicated by blue arrows. Inset shows the movement of the side chain of Trp-400<sup>7,35</sup>.

## DISCUSSION

BQCA demonstrates a number of unique properties relative to previously described allosteric ligands of the mAChR family, including an exquisite selectivity for  $M_1$  mAChRs over other subtypes and a mechanism of action that appears in strict accordance with a two-state model of receptor activity, such that it is a positive modulator of agonists but a negative modulator of antagonists/inverse agonists (16, 17). Moreover, the

compound is active *in vivo* (18, 53), providing proof of concept for the validity of allosteric targeting of  $M_1$  mAChRs in the treatment of CNS disorders, and it has been the focus of numerous structure-activity studies (15, 54) aimed at improving its “druggability” and affinity. However, it is now apparent that allosteric modulators can achieve selectivity by more than one mechanism, *i.e.* at the level of structural divergence of an allosteric pocket across GPCR subtypes or via selective cooperativ-

ity at a given subtype despite acting at a “conserved” allosteric site (14). The latter paradigm is best exemplified by the mAChRs, in which are all characterized by an extracellular vestibule that can be recognized by structurally diverse allosteric ligands (12, 13). To better understand the basis of the selectivity of BQCA, we combined mutagenesis with mathematical and molecular modeling to identify potential structural contributors to its binding pocket and its ability to allosterically modulate the binding and signaling of the prototypical orthosteric agonist CCh.

Although no affinity values could be obtained for BQCA at residues where allosteric modulation was abolished (Tyr-106<sup>3,33</sup>, Trp-157<sup>4,57</sup> and Tyr-381<sup>6,51</sup> and Trp-400<sup>7,35</sup>), our study identified residues of the  $M_1$  mAChR that contribute to the following: (i) the binding affinity of the modulator; (ii) the cooperativity between the modulator and the orthosteric agonist CCh; (iii) the ability of the modulator to drive the receptor into an active state, and (iv) enhancement of the binding affinity of BQCA.

Alanine substitution of a number of residues from various regions in the receptor caused a decrease in the cooperativity between BQCA and CCh in binding and functional interaction studies (Figs. 4 and 8 and Tables 2 and 4). Such reductions in cooperativity resulted either from mutation of residues that form the proposed allosteric binding pocket or residues conformationally linked to the allosteric site and thus needed for the transmission of cooperativity or receptor activation upon ligand binding. Our MD simulations support this hypothesis and the experimental findings. As shown in Fig. 9, the proposed BQCA pocket is topographically distinct from the orthosteric binding site, and these two sites are separated by a shelf of aromatic residues. The residues that are predicted to form the BQCA binding pocket, mainly from ECL2 (Tyr-179), TMII (Tyr-85<sup>2,64</sup>), and TMVII (Trp-400<sup>7,35</sup>) or those whose mutation to alanine cause significant decreases in cooperativity (Phe-182, Glu-397<sup>7,32</sup>, and Glu-401<sup>7,36</sup>), are equivalent to residues that have been implicated in the binding of several allosteric ligands at mAChRs, as follows: (i) the action of gallamine and the allosteric antagonist MT7 at the  $M_1$  mAChR (40, 47); (ii) the action of LY2033298 at the  $M_4$  mAChR (34), and (iii) the action of  $C_{7/3}$ -phth, gallamine, alcuronium, McN-A-343, alkane-bisammonium, and caracurine V-type allosteric modulators at the  $M_2$  mAChR (13, 35, 42, 55–57).

The only residue in the proposed BQCA binding pocket that leads to complete loss of modulation in both functional and binding assays is Trp-400<sup>7,35</sup>. This suggests that the  $\pi$ - $\pi$  interaction of the benzylic pendant of BQCA and the aromatic side chain of Trp-400<sup>7,35</sup> makes either a major contribution to BQCA binding and/or maintaining the structure of the local binding pocket of BQCA. Other residues, such as Tyr-179, Tyr-82<sup>2,61</sup>, and Tyr-85<sup>2,64</sup>, while predicted in our MD simulations to interact with BQCA, appear to have a predominant role in the transmission of BQCA's modulator action on orthosteric ligands such that their mutation to alanine impairs the transmission of cooperativity but does not lead to a significant loss of binding affinity. Of interest, a recent molecular dynamics study identified two binding centers in the extracellular vestibule of the  $M_2$  mAChR, each defined by a pair of aromatic residues

(center 1, Tyr-177<sup>ECL2</sup> and Trp<sup>7,35</sup>; center 2, Tyr<sup>2,61</sup> and Tyr<sup>2,64</sup>) (13). It is noteworthy that we identified these residues as key contributors for the binding and function of BQCA. Furthermore, Tyr<sup>2,64</sup> and Trp<sup>7,35</sup> are conserved across all mAChR receptor subtypes; Tyr<sup>2,61</sup> is conserved across all but the  $M_3$  mAChR (where it is replaced by a similarly aromatic phenylalanine residue), and Tyr-179 is only present at the  $M_1$  and  $M_2$  mAChRs but is a phenylalanine at the  $M_3$  and  $M_4$  mAChRs. This is consistent with BQCA sharing a common binding site with other prototypical mAChR allosteric modulators. Glu-397<sup>7,32</sup> and Glu-401<sup>7,36</sup> are not conserved across the mAChR family and were predicted by our modeling experiments to make minimal interaction with BQCA. Mutation of these residues had no effect on BQCA binding affinity but decreased cooperativity with CCh. This suggests that such residues may govern the subtype-specific cooperative effect of BQCA upon orthosteric ligand binding from a conserved allosteric pocket.

The observation of a correlation between the change in CCh binding affinity ( $pK_I$ ) and BQCA binding affinity ( $pK_B$ ) is entirely consistent with our previous description of the mechanism of BQCA within the confines of a strict two-state model (Fig. 5) (17). Furthermore, the finding that the orthosteric site residues shown in Fig. 9B lead to complete loss (Y106<sup>3,33</sup>A, W157<sup>4,57</sup>A, and Y381<sup>6,51</sup>A), or significant reduction (D105<sup>3,32</sup>A) in the binding cooperativity between CCh and BQCA is a striking example of a conformationally linked mechanism for the transmission of cooperativity. The efficacy of CCh was severely reduced when each of these residues was mutated, but this was “rescued” by BQCA. Furthermore, these additional functional interaction data confirmed the ability of BQCA to bind to this set of mutant receptors, a conclusion that could not be drawn from the binding data alone. This highlights the importance of using both binding and functional assays to characterize the effect of mutations upon allosteric ligand function.

Given that an analogous observation was made for the action of the positive allosteric modulator, LY2033298, at a functionally impaired  $M_4$  mAChR double mutant containing the Y113<sup>3,33</sup>C (48) or the D112<sup>3,32</sup>E mutation (33), our results indicate that BQCA may share similarities in mechanism of action and may bind to a site that is spatially conserved between the  $M_4$  the  $M_1$  mAChRs. However, the very high selectivity of BQCA for the  $M_1$  mAChR (as opposed to LY2033298 that acts at both the  $M_2$  and  $M_4$  mAChRs) indicates that although the allosteric sites of these two ligands share some epitopes, they may engage additional distinct residues either in their mode of binding or transmission of cooperativity to the orthosteric site.

In addition to regions of the receptor that were primarily important for the binding of BQCA and transmission of cooperativity, we also identified mutations that caused a significant enhancement in the affinities of both CCh and BQCA (Q181A, F374<sup>6,44</sup>A, and W405<sup>7,40</sup>A). Previous studies have reported increases in CCh affinity at Q181A (36, 40), whereas others have reported constitutive receptor activity when residues 6.44 and 7.40 are mutated to alanine (41, 43). The movement of the side chain of Phe<sup>6,44</sup> is coupled to an outward movement of TMVI upon  $\beta_2$ -adrenergic receptor activation (58), and it has been reported to be a microswitch in GPCR activation (50). It

## Structure-Function Analysis of $M_1$ Receptor Allostery

has also been suggested that Trp-405<sup>7,40</sup> restricts thermal motions of the extracellular domain of TMVII of mAChRs (3).

In summary, we have identified key regions in the  $M_1$  mAChR that are involved in the binding and signaling of CCh and BQCA, and in the transmission of cooperativity between the orthosteric and an allosteric binding site. We propose that some of the structural determinants of these effects are analogous to those of other family A GPCRs, but the unique selectivity of BQCA arises from the additional involvement of nonconserved residues (e.g. Glu-397<sup>7,32</sup> and Glu-401<sup>7,36</sup>) and/or selective cooperativity with agonists at the  $M_1$  mAChR. Therefore, our results provide further understanding of the structural basis of allosteric modulation that may be of general application to GPCR drug discovery and that can help guide the more rational design of allosteric ligands that target this distinct site. In particular, they challenge an important concept often associated with allosteric targeting of GPCRs, namely that selective modulators gain subtype selectivity through their binding to a site that is not conserved across a receptor subfamily. Rather, as highlighted in our study, selective cooperativity via interaction with a conserved allosteric site is also possible. Given the increasing number of GPCR crystal structures now being solved, it should thus be appreciated that structure-based drug design using *in silico* screening for novel allosteric modulators will not, in and of itself, guarantee a desired level of selectivity without complementation by additional structure-function approaches as described herein.

*Acknowledgments*—We are grateful to Dr. Ann Stewart for generating some of the  $M_1$  mAChR mutants and Briana J. Davie for the synthesis of BQCA.

### REFERENCES

1. Venkatakrishnan, A. J., Deupi, X., Lebon, G., Tate, C. G., Schertler, G. F., and Babu, M. M. (2013) Molecular signatures of G-protein-coupled receptors. *Nature* **494**, 185–194
2. Lagerström, M. C., and Schiöth, H. B. (2008) Structural diversity of G protein-coupled receptors and significance for drug discovery. *Nat. Rev. Drug Discov.* **7**, 339–357
3. Hulme, E. C. (2013) GPCR activation: a mutagenic spotlight on crystal structures. *Trends Pharmacol. Sci.* **34**, 67–84
4. Stevens, R. C., Cherezov, V., Katritch, V., Abagyan, R., Kuhn, P., Rosen, H., and Wüthrich, K. (2013) The GPCR Network: a large-scale collaboration to determine human GPCR structure and function. *Nat. Rev. Drug Discov.* **12**, 25–34
5. Miao, Y., Nichols, S. E., Gasper, P. M., Metzger, V. T., and McCammon, J. A. (2013) Activation and dynamic network of the M2 muscarinic receptor. *Proc. Natl. Acad. Sci. U.S.A.* **110**, 10982–10987
6. Wacker, D., Wang, C., Katritch, V., Han, G. W., Huang, X.-P., Vardy, E., McCorvy, J. D., Jiang, Y., Chu, M., Siu, F. Y., Liu, W., Xu, H. E., Cherezov, V., Roth, B. L., and Stevens, R. C. (2013) Structural features for functional selectivity at serotonin receptors. *Science* **340**, 615–619
7. Haga, K., Kruse, A. C., Asada, H., Yurugi-Kobayashi, T., Shiroishi, M., Zhang, C., Weis, W. I., Okada, T., Kobilka, B. K., Haga, T., and Kobayashi, T. (2012) Structure of the human M2 muscarinic acetylcholine receptor bound to an antagonist. *Nature* **482**, 547–551
8. Conn, P. J., Christopoulos, A., and Lindsley, C. W. (2009) Allosteric modulators of GPCRs: a novel approach for the treatment of CNS disorders. *Nat. Rev. Drug Discov.* **8**, 41–54
9. Conn, P. J., Jones, C. K., and Lindsley, C. W. (2009) Subtype-selective allosteric modulators of muscarinic receptors for the treatment of CNS disorders. *Trends Pharmacol. Sci.* **30**, 148–155
10. Tan, Q., Zhu, Y., Li, J., Chen, Z., Han, G. W., Kufareva, I., Li, T., Ma, L., Fenalti, G., Li, J., Zhang, W., Xie, X., Yang, H., Jiang, H., Cherezov, V., Liu, H., Stevens, R. C., Zhao, Q., and Wu, B. (2013) Structure of the CCR5 chemokine receptor–HIV entry inhibitor maraviroc complex. *Science* **341**, 1387–1390
11. Kruse, A. C., Hu, J., Pan, A. C., Arlow, D. H., Rosenbaum, D. M., Rosemond, E., Green, H. F., Liu, T., Chae, P. S., Dror, R. O., Shaw, D. E., Weis, W. I., Wess, J., and Kobilka, B. K. (2012) Structure and dynamics of the M3 muscarinic acetylcholine receptor. *Nature* **482**, 552–556
12. De Amici, M., Dallanoce, C., Holzgrabe, U., Tränkle, C., and Mohr, K. (2010) Allosteric ligands for G protein-coupled receptors: A novel strategy with attractive therapeutic opportunities. *Med. Res. Rev.* **30**, 463–549
13. Dror, R. O., Green, H. F., Valant, C., Borhani, D. W., Valcourt, J. R., Pan, A. C., Arlow, D. H., Canals, M., Lane, J. R., Rahmani, R., Baell, J. B., Sexton, P. M., Christopoulos, A., and Shaw, D. E. (2013) Structural basis for modulation of a G-protein-coupled receptor by allosteric drugs. *Nature* **503**, 295–299
14. Valant, C., Felder, C. C., Sexton, P. M., and Christopoulos, A. (2012) Probe dependence in the allosteric modulation of a G protein-coupled receptor: implications for detection and validation of allosteric ligand effects. *Mol. Pharmacol.* **81**, 41–52
15. Davie, B. J., Christopoulos, A., and Scammells, P. J. (2013) Development of M1 mAChR allosteric and bitopic ligands: prospective therapeutics for the treatment of cognitive deficits. *ACS Chem. Neurosci.* **4**, 1026–1048
16. Abdul-Ridha, A., Lane, J. R., Sexton, P. M., Canals, M., and Christopoulos, A. (2013) Allosteric modulation of a chemogenetically modified G protein-coupled receptor. *Mol. Pharmacol.* **83**, 521–530
17. Canals, M., Lane, J. R., Wen, A., Scammells, P. J., Sexton, P. M., and Christopoulos, A. (2012) A Monod-Wyman-Changeux mechanism can explain G protein-coupled receptor (GPCR) allosteric modulation. *J. Biol. Chem.* **287**, 650–659
18. Ma, L., Seager, M. A., Seager, M., Wittmann, M., Jacobson, M., Bickel, D., Burno, M., Jones, K., Graufelds, V. K., Xu, G., Pearson, M., McCampbell, A., Gaspar, R., Shughrue, P., Danziger, A., Regan, C., Flick, R., Pascarella, D., Garson, S., Doran, S., Kretsoulas, C., Veng, L., Lindsley, C. W., Shipe, W., Kuduk, S., Sur, C., Kinney, G., Seabrook, G. R., and Ray, W. J. (2009) Selective activation of the M1 muscarinic acetylcholine receptor achieved by allosteric potentiation. *Proc. Natl. Acad. Sci. U.S.A.* **106**, 15950–15955
19. Black, J. W., and Leff, P. (1983) Operational models of pharmacological agonism. *Proc. R. Soc. Lond. B Biol. Sci.* **220**, 141–162
20. Leach, K., Sexton, P. M., and Christopoulos, A. (2007) Allosteric GPCR modulators: taking advantage of permissive receptor pharmacology. *Trends Pharmacol. Sci.* **28**, 382–389
21. Thompson, J. D., Gibson, T. J., Plewniak, F., Jeanmougin, F., and Higgins, D. G. (1997) The CLUSTAL\_X windows interface: flexible strategies for multiple sequence alignment aided by quality analysis tools. *Nucleic Acids Res.* **25**, 4876–4882
22. Rasmussen, S. G., Choi, H. J., Fung, J. J., Pardon, E., Casarosa, P., Chae, P. S., Devree, B. T., Rosenbaum, D. M., Thian, F. S., Kobilka, T. S., Schnapp, A., Konetzki, I., Sunahara, R. K., Gellman, S. H., Pautsch, A., Steyaert, J., Weis, W. I., and Kobilka, B. K. (2011) Structure of a nanobody-stabilized active state of the  $\beta_2$  adrenoceptor. *Nature* **469**, 175–180
23. Ballesteros, J. A., and Weinstein, H. (1995) In *Methods in Neurosciences* (Stuart, C. S., ed) pp. 366–428, Academic Press, New York
24. Sali, A., and Blundell, T. L. (1993) Comparative protein modelling by satisfaction of spatial restraints. *J. Mol. Biol.* **234**, 779–815
25. Duan, Y., Wu, C., Chowdhury, S., Lee, M. C., Xiong, G., Zhang, W., Yang, R., Cieplak, P., Luo, R., Lee, T., Caldwell, J., Wang, J., and Kollman, P. (2003) A point-charge force field for molecular mechanics simulations of proteins based on condensed-phase quantum mechanical calculations. *J. Comput. Chem.* **24**, 1999–2012
26. Wang, J., Wolf, R. M., Caldwell, J. W., Kollman, P. A., and Case, D. A. (2004) Development and testing of a general amber force field. *J. Comput. Chem.* **25**, 1157–1174
27. Phillips, J. C., Braun, R., Wang, W., Gumbart, J., Tajkhorshid, E., Villa, E., Chipot, C., Skeel, R. D., Kalé, L., and Schulten, K. (2005) Scalable molecular dynamics with NAMD. *J. Comput. Chem.* **26**, 1781–1802

28. Shonberg, J., Herenbrink, C. K., López, L., Christopoulos, A., Scammells, P. J., Capuano, B., and Lane, J. R. (2013) A structure-activity analysis of biased agonism at the dopamine D2 receptor. *J. Med. Chem.* **56**, 9199–9221
29. Motulsky H. J., and Christopoulos, A. (2003) Fitting models to biological data using linear and nonlinear regression. *A Practical Guide to Curve Fitting*, GraphPad Software Inc., San Diego
30. Leach, K., Loiacono, R. E., Felder, C. C., McKinzie, D. L., Mogg, A., Shaw, D. B., Sexton, P. M., and Christopoulos, A. (2010) Molecular mechanisms of action and *in vivo* validation of an M4 muscarinic acetylcholine receptor allosteric modulator with potential antipsychotic properties. *Neuropsychopharmacology* **35**, 855–869
31. Kenakin, T., and Christopoulos, A. (2013) Signalling bias in new drug discovery: detection, quantification and therapeutic impact. *Nat. Rev. Drug Discov.* **12**, 205–216
32. Christopoulos, A. (1998) Assessing the distribution of parameters in models of ligand-receptor interaction: to log or not to log. *Trends Pharmacol. Sci.* **19**, 351–357
33. Leach, K., Davey, A. E., Felder, C. C., Sexton, P. M., and Christopoulos, A. (2011) The role of transmembrane domain 3 in the actions of orthosteric, allosteric, and atypical agonists of the m4 muscarinic acetylcholine receptor. *Mol. Pharmacol.* **79**, 855–865
34. Nawaratne, V., Leach, K., Felder, C. C., Sexton, P. M., and Christopoulos, A. (2010) Structural determinants of allosteric agonism and modulation at the M4 muscarinic acetylcholine receptor: identification of ligand-specific and global activation mechanisms. *J. Biol. Chem.* **285**, 19012–19021
35. Valant, C., Gregory, K. J., Hall, N. E., Scammells, P. J., Lew, M. J., Sexton, P. M., and Christopoulos, A. (2008) A novel mechanism of G protein-coupled receptor functional selectivity. Muscarinic partial agonist McN-A-343 as a bitopic orthosteric/allosteric ligand. *J. Biol. Chem.* **283**, 29312–29321
36. Goodwin, J. A., Hulme, E. C., Langmead, C. J., and Tehan, B. G. (2007) Roof and floor of the muscarinic binding pocket: variations in the binding modes of orthosteric ligands. *Mol. Pharmacol.* **72**, 1484–1496
37. Lu, Z.-L., and Hulme, E. C. (1999) The functional topography of transmembrane domain 3 of the M1 muscarinic acetylcholine receptor, revealed by scanning mutagenesis. *J. Biol. Chem.* **274**, 7309–7315
38. Lu, Z.-L., Saldanha, J. W., and Hulme, E. C. (2001) Transmembrane domains 4 and 7 of the M1 muscarinic acetylcholine receptor are critical for ligand binding and the receptor activation switch. *J. Biol. Chem.* **276**, 34098–34104
39. Avlani, V. A., Langmead, C. J., Guida, E., Wood, M. D., Tehan, B. G., Herdon, H. J., Watson, J. M., Sexton, P. M., and Christopoulos, A. (2010) Orthosteric and allosteric modes of interaction of novel selective agonists of the M1 muscarinic acetylcholine receptor. *Mol. Pharmacol.* **78**, 94–104
40. Matsui, H., Lazareno, S., and Birdsall, N. J. (1995) Probing of the location of the allosteric site on m1 muscarinic receptors by site-directed mutagenesis. *Mol. Pharmacol.* **47**, 88–98
41. Daval, S. B., Kellenberger, E., Bonnet, D., Utard, V., Galzi, J. L., and Ilien, B. (2013) Exploration of the orthosteric/allosteric interface in human m1 muscarinic receptors by bitopic fluorescent ligands. *Mol. Pharmacol.* **84**, 71–85
42. Prilla, S., Schrobang, J., Ellis, J., Höltje, H.-D., and Mohr, K. (2006) Allosteric interactions with muscarinic acetylcholine receptors: complex role of the conserved tryptophan M2422Trp in a critical cluster of amino acids for baseline affinity, subtype selectivity, and cooperativity. *Mol. Pharmacol.* **70**, 181–193
43. Spalding, T. A., Burstein, E. S., Henderson, S. C., Ducote, K. R., and Brann, M. R. (1998) Identification of a ligand-dependent switch within a muscarinic receptor. *J. Biol. Chem.* **273**, 21563–21568
44. Hulme, E. C., Lu, Z. L., Saldanha, J. W., and Bee, M. S. (2003) Structure and activation of muscarinic acetylcholine receptors. *Biochem. Soc. Trans.* **31**, 29–34
45. Lebois, E. P., Bridges, T. M., Lewis, L. M., Dawson, E. S., Kane, A. S., Xiang, Z., Jadhav, S. B., Yin, H., Kennedy, J. P., Meiler, J., Niswender, C. M., Jones, C. K., Conn, P. J., Weaver, C. D., and Lindsley, C. W. (2010) Discovery and characterization of novel subtype-selective allosteric agonists for the investigation of M(1) receptor function in the central nervous system. *ACS Chem. Neurosci.* **1**, 104–121
46. May, L. T., Avlani, V. A., Langmead, C. J., Herdon, H. J., Wood, M. D., Sexton, P. M., and Christopoulos, A. (2007) Structure-function studies of allosteric agonism at M2 muscarinic acetylcholine receptors. *Mol. Pharmacol.* **72**, 463–476
47. Marquer, C., Fruchart-Gaillard, C., Letellier, G., Marcon, E., Mourier, G., Zinn-Justin, S., Ménez, A., Servent, D., and Gilquin, B. (2011) Structural model of ligand-G protein-coupled receptor (GPCR) complex based on experimental double mutant cycle data. *J. Biol. Chem.* **286**, 31661–31675
48. Nawaratne, V., Leach, K., Suratman, N., Loiacono, R. E., Felder, C. C., Armbruster, B. N., Roth, B. L., Sexton, P. M., and Christopoulos, A. (2008) New insights into the function of M4 muscarinic acetylcholine receptors gained using a novel allosteric modulator and a DREADD (designer receptor exclusively activated by a designer drug). *Mol. Pharmacol.* **74**, 1119–1131
49. Cherezov, V., Rosenbaum, D. M., Hanson, M. A., Rasmussen, S. G., Thian, F. S., Kobilka, T. S., Choi, H. J., Kuhn, P., Weis, W. I., Kobilka, B. K., and Stevens, R. C. (2007) High-resolution crystal structure of an engineered human  $\beta$ 2-adrenergic G protein-coupled receptor. *Science* **318**, 1258–1265
50. Valentin-Hansen, L., Holst, B., Frimurer, T. M., and Schwartz, T. W. (2012) PheVI:09 (Phe6.44) as a sliding microswitch in seven-transmembrane (7TM) G protein-coupled receptor activation. *J. Biol. Chem.* **287**, 43516–43526
51. Choe, H. W., Kim, Y. J., Park, J. H., Morizumi, T., Pai, E. F., Krauss, N., Hofmann, K. P., Scheerer, P., and Ernst, O. P. (2011) Crystal structure of metarhodopsin II. *Nature* **471**, 651–655
52. Lebon, G., Warne, T., Edwards, P. C., Bennett, K., Langmead, C. J., Leslie, A. G., and Tate, C. G. (2011) Agonist-bound adenosine A2A receptor structures reveal common features of GPCR activation. *Nature* **474**, 521–525
53. Shirey, J. K., Brady, A. E., Jones, P. J., Davis, A. A., Bridges, T. M., Kennedy, J. P., Jadhav, S. B., Menon, U. N., Xiang, Z., Watson, M. L., Christian, E. P., Doherty, J. J., Quirk, M. C., Snyder, D. H., Lah, J. J., Levey, A. L., Nicolle, M. M., Lindsley, C. W., and Conn, P. J. (2009) A selective allosteric potentiator of the M1 muscarinic acetylcholine receptor increases activity of medial prefrontal cortical neurons and restores impairments in reversal learning. *J. Neurosci.* **29**, 14271–14286
54. Mistry, S. N., Valant, C., Sexton, P. M., Capuano, B., Christopoulos, A., and Scammells, P. J. (2013) Synthesis and pharmacological profiling of analogues of benzyl quinolone carboxylic acid (BQCA) as allosteric modulators of the M1 muscarinic receptor. *J. Med. Chem.* **56**, 5151–5172
55. Huang, X. P., Prilla, S., Mohr, K., and Ellis, J. (2005) Critical amino acid residues of the common allosteric site on the M2 muscarinic acetylcholine receptor: more similarities than differences between the structurally divergent agents gallamine and bis(ammonio)alkane-type hexamethylene-bis-[dimethyl-(3-phthalimidopropyl)ammonium]dibromide. *Mol. Pharmacol.* **68**, 769–778
56. May, L. T., Leach, K., Sexton, P. M., and Christopoulos, A. (2007) Allosteric modulation of G protein-coupled receptors. *Annu. Rev. Pharmacol. Toxicol.* **47**, 1–51
57. Voigtländer, U., Jöhren, K., Mohr, M., Raasch, A., Tränkle, C., Buller, S., Ellis, J., Höltje, H. D., and Mohr, K. (2003) Allosteric site on muscarinic acetylcholine receptors: identification of two amino acids in the muscarinic M2 receptor that account entirely for the M2/M5 subtype selectivities of some structurally diverse allosteric ligands in *N*-methylscopolamine-occupied receptors. *Mol. Pharmacol.* **64**, 21–31
58. Rasmussen, S. G., DeVree, B. T., Zou, Y., Kruse, A. C., Chung, K. Y., Kobilka, T. S., Thian, F. S., Chae, P. S., Pardon, E., Calinski, D., Mathiesen, J. M., Shah, S. T., Lyons, J. A., Caffrey, M., Gellman, S. H., Steyaert, J., Skiniotis, G., Weis, W. I., Sunahara, R. K., and Kobilka, B. K. (2011) Crystal structure of the  $\beta$ 2 adrenergic receptor-Gs protein complex. *Nature* **477**, 549–555